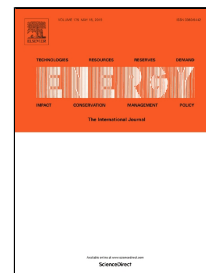


# Accepted Manuscript

The impact of climatic extreme events on the feasibility of fully renewable power systems: a case study for Sweden

Stefan Höltinger, Christian Mikovits, Johannes Schmidt, Johann Baumgartner, Berit Arheimer, Göran Lindström, Elisabeth Wetterlund



PII: S0360-5442(19)30761-3  
DOI: 10.1016/j.energy.2019.04.128  
Reference: EGY 15157  
To appear in: *Energy*  
Received Date: 23 October 2018  
Accepted Date: 20 April 2019

Please cite this article as: Stefan Höltinger, Christian Mikovits, Johannes Schmidt, Johann Baumgartner, Berit Arheimer, Göran Lindström, Elisabeth Wetterlund, The impact of climatic extreme events on the feasibility of fully renewable power systems: a case study for Sweden, *Energy* (2019), doi: 10.1016/j.energy.2019.04.128

This is a PDF file of an unedited manuscript that has been accepted for publication. As a service to our customers we are providing this early version of the manuscript. The manuscript will undergo copyediting, typesetting, and review of the resulting proof before it is published in its final form. Please note that during the production process errors may be discovered which could affect the content, and all legal disclaimers that apply to the journal pertain.

# The impact of climatic extreme events on the feasibility of fully renewable power systems: a case study for Sweden

Stefan Höltinger<sup>a</sup>, Christian Mikovits<sup>a</sup>, Johannes Schmidt<sup>a</sup>, Johann Baumgartner<sup>a</sup>, Berit Arheimer<sup>b</sup>, Göran Lindström<sup>b</sup>, Elisabeth Wetterlund<sup>c,d</sup>

<sup>a</sup> Institute for Sustainable Economic Development, University of Natural Resources and Life Science Vienna, Austria

<sup>b</sup> Swedish Meteorological and Hydrological Institute (SMHI), Norrköping, Sweden

<sup>c</sup> Energy Engineering, Division of Energy Science, Luleå University of Technology, 971 87 Luleå, Sweden

<sup>d</sup> International Institute for Applied Systems Analysis (IIASA), A-2361 Laxenburg, Austria

## Abstract

Long term time series of variable renewable energy (VRE) generation and electricity demand (load) provide important insights into the feasibility of fully renewable power systems. The coverage of energy statistics is usually too short or the temporal resolution too low to study effects related to interannual variability or the impact of climatic extreme events. We use time series simulated from climate data to assess the frequency, duration, and magnitude of extreme residual load events of two fully renewable power scenarios with a share of VRE generation (wind and solar PV) of about 50% for the case of Sweden. We define residual load as load – wind – PV – nuclear generation. Extreme residual load events are events that exceed the balancing or ramping capacities of the current power system. For our analysis, we use 29 years of simulated river runoff and wind and PV generation. Hourly load is derived from MERRA reanalysis temperature data by applying statistical models. Those time series are used along with historic capacity and ramping restrictions of hydro and thermal power plants in an optimization model to minimize extreme residual load events. Our analysis shows that even highly flexible power systems, as the Swedish one, are affected by climatic extreme events if they increase their VRE shares. Replacing current nuclear power capacities by wind power results on average in three extreme residual load events per year that exceed the current power system's flexibility. Additional PV generation capacities instead of wind increase the number of extreme residual load events by about 4 %, as most events occur during the winter month when solar generation is close to zero and thus not able to counterbalance low wind events. Contrarily, overproduction and the need to curtail VRE generation become more pressing with higher shares of PV. In the discussion we highlight measures that could provide additional balancing capabilities to cope with the more frequent and severe residual load events in a fully renewable power system with high shares of VRE generation.

**Highlights:**

- Load during winter is negatively correlated with wind power and natural river runoff
- Annual residual loads vary between 51 and 72 TWh in a fully renewable power system
- Two out of three years exceed the balancing capacities of the current power system
- The longest extreme residual load event lasts 18 hours with a maximum lack of capacity of 4 GW
- Additional flexibility measures can avoid loss of load events in fully renewable power systems

## 1 Introduction

The transition to fully renewable power systems is an important prerequisite for limiting adverse long-term impacts of climate change [1]. Wind power and solar photovoltaics (PV) have experienced significant cost reduction and growth rates in recent years [2,3]. One major concern for large shares of variable renewable energy (VRE), such as wind and PV, is still their variable (intermittent) nature that increases the vulnerability of power systems to extreme climatic events. The frequency and duration of extreme production events in fully renewable power systems is of high relevance, as power systems are designed to endure maximum load and peak generation capacities contribute significantly to the overall systems cost.

Critics warn that periods of persistent low VRE generation might threaten grid stability and exceed the balancing capabilities of current power systems [4]. Therefore, power system studies that aim at determining the optimal mix of wind and solar in future power systems increasingly use long-term time series to avoid criticism that results may be valid only for the given year(s), while not being feasible for years with extreme climatic conditions [5]. This is important as VRE generation and electricity demand exhibit not only seasonal but also considerable interannual variation.

Recent works, therefore, use global reanalysis data-sets, such as the MERRA reanalysis data [6] to derive long-term time series of VRE generation. These time series provide an important input for the growing body of literature that assesses the variability of VRE and its impacts on the balancing power as well as storage and transmission capacity needs of power systems with high shares of up to 100% renewables. The flexibility requirements of power systems on country or continental level are usually assessed by analysing net load variations [5,7–10]. For a detailed discussion of fully renewable power scenarios see [11]. Residual load refers to the difference between load and VRE generation and equals the amount of electricity that must be provided by dispatchable power plants, storage or demand side management options. While most of the studies argue that it is necessary to include long-term time series of VRE generation to account for interannual variations of VRE generation, most of them rely on historical data for electricity demand covering only representative days [12] or one or two [7,13,14] up to 5 [8] and 10 [5] years. However, climatic conditions affect electricity demand in a similar way as VRE generation. For assessing extreme residual load events, it is therefore crucial to use long-term time series for load as well, as low VRE generation events might be easily balanced during mild winter days but become a problem during cold winter days with high heating demand. In this article we aim to overcome this limitation by using MERRA temperature data to simulate 35 years of hourly temperature dependent load. Based on the simulated time series for VRE generation and load we assess the frequency and magnitude of extreme residual load events and the implications for balancing capacities for Sweden as a case study. While previous studies mostly use techno-economic assumptions to describe the technical capabilities of the system (such as ramping), we, in contrast, derive historical capabilities from empirical data and use it in our modelling approach.

The most important resource for balancing extreme residual load events in Sweden is hydropower, which contributes to over 40% of today's electricity production in Sweden [15]. Hydropower plants can be operated very flexibly to provide ramping capacities for short term fluctuations of VRE. Beyond that, Sweden has a large amount of hydro reservoirs with a total

capacity of about 33 TWh [16]. This is about a quarter of the annual electricity demand and provides enough storage capacity to balance seasonal and, to some extent, also interannual fluctuations of VRE. However, analogous to VRE, hydropower generation may vary considerably between wet and dry years. Currently, Sweden still produces 40% of its electricity from nuclear power plants [15]. While the proposed target for 2040 is 100% renewable electricity production, there is currently no political decision regarding nuclear phase-out in place [17]. However, nuclear power must cover its own costs, including costs for disposal of spent fuel and nuclear waste, without subsidies. Further, several currently operating plants need major investment in order to meet safety requirements. For these reasons, nuclear power may be expected to be, partly or fully, phased out during the coming decades, which could boost the share of VRE and initiate the transition to a fully renewable power system.

In this article, we assess the feasibility of two scenarios for a fully renewable power supply in Sweden by considering long-term climatic variations, using continuous hourly time-series from 1986 to 2014. We address several aspects that affect the short- and long-term flexibility needs of balancing and storage capacities. Our aim is to provide a better understanding of current, available system flexibility when taking into account climatic extreme events and thus we do not include all available flexibility options [18]. Considering all these options is typically done when assessing investments into new options for integrating renewables such as in [12,14]. This is not our aim, instead we assess (1) the current balancing and ramping capacities in the system and how they are affected by a high penetration of VRE under nuclear phase-out in Sweden, (2) the frequency and magnitude of extreme residual load events and the capability of the system to deal with them, and (3) the inter-annual variations in renewable supply and electricity demand, possible systematic relationships between these variables, and resulting challenges for the power system. For this purpose, we generate residual load time series for a 29-year period by subtracting simulated VRE generation from simulated load. Based on those time series we assess how the hydro-thermal power system can cover residual load. For that purpose, a stylized optimization model of the Swedish hydro-power system is used to optimize hydropower production.

## 2 Data and Methods

We assess extreme residual load events in two fully renewable power scenarios with a share of VRE generation (wind and solar PV) of about 50%. For that purpose, we use 29 years, from 1986 to 2014, of simulated wind and PV generation in conjunction with statistical models to derive hourly load from MERRA reanalysis temperature data. The time series are used along with historic capacity and ramping restriction in an optimization model to assess the flexibility that can be provided by hydro and thermal power plants. In this section, we describe two alternatives for a fully renewable power supply, the data and models used to derive time series for VRE generation and load, as well as the optimization model used to assess the maximum flexibility that can be provided by hydro and thermal power plants.

### 2.1 Scenarios for a fully renewable power supply with VRE

In this paper we focus on assessing the impact of fully renewable power scenarios on the residual load variability and its implications for the flexibility needs of the power system. Therefore, we compare extreme residual load events in the current power system with two

fully renewable power scenarios that assume that the current nuclear power generation of about 60 TWh annually is phased out and replaced with VRE generation capacities (see Table 1). The reference scenario uses historic generation and load data from 2007 to 2016 and provides a reference for the fully renewable power scenarios. In this case, residual load refers to the difference between load and VRE plus nuclear power. The Wind scenario assumes that nuclear power is replaced by wind energy alone - adding up to an installed wind capacity of 19.2 GW or an average annual wind power output of about 70 TWh, which is well in line with estimates of Swedish wind power potential by Byman et. al. [16]. The wind+PV scenario assumes the same VRE mix as the “More solar and wind” alternative in the IVA Electricity Crossroads project [16] with 55 TWh wind (15.1 GW installed capacity) and 15 TWh solar power (16.9 GW installed capacity). Capacity factors of wind power plants increase in the scenarios, due to assumed technological improvements and a higher share of offshore wind power. Both of our fully renewable scenarios assume that load and generation capacities of other technologies (i.e. hydropower and thermal) remain constant. Future thermal generation though is assumed to rely only on biomass resources to guarantee a fully renewable electricity supply. Imports and exports are not explicitly considered in the model but will be discussed along with other balancing options in the discussion section. Differences in mean annual power demand stem from the fact that demand in the reference scenario is observed, while demand in the renewable scenarios is derived from a statistical model (see below).

*Table 1: Mean annual generation and power demand (TWh/y) from 2007 to 2014 and installed capacities (GW) as this period is available for both simulated and observed data*

	Reference scenario		Wind scenario		Wind+PV scenario	
	TWh/y	GW	TWh/y	GW	TWh/y	GW
Load (power demand)	131.1		129.6		129.6	
Hydro	67.0	16.2	64.1	16.2	64.1	16.2
Nuclear	59.7	9.5	0	0	0	
Wind	11.6*	5.4*	69.3	19.2	54.4	15.1
PV	< 0.1	< 0.1	0	0	14.9	16.9
Thermal (biomass)	9.7	8.4	9.7	8.4	9.7	8.4

\* values for wind in the reference scenario for 2014 only

## 2.2 Hydro runoff and variable renewable energy generation data sets

In order to assess the balancing capabilities of Swedish hydropower for short-term balancing (hourly fluctuations) as well as seasonal variations, we use simulated time series for river discharge from the hydrological catchment model S-HYPE. The model simulates water flow from precipitation through soil, river and lakes to the river outlet [19,20] and provides daily time series of natural and corrected river runoff. The natural runoff simulates river runoff without human interference such as hydropower. The corrected discharge is modelled using regulation routines but replaced by observations where such are available. Up to now, hydropower plants have been operated to respond to changing electricity demand. Higher shares of VRE generation will change these prevailing hydro and thermal power generation patterns as they will increasingly have to balance fluctuations of wind and solar generation. Thus, it is not meaningful to use the corrected HYPE runoff data for simulating hydropower

generation in fully renewable power systems. Instead, we implement the natural runoff data in a residual load balancing optimization model (see Section 2.4).

For **wind power** assessments, it has become common practice to use wind speed time series from reanalysis data, which is then converted into power output using approximations of standard power curves [21]. However, using output from reanalysis models may lead to significant spatial bias and overestimate wind output by up to 50% (e.g. in Northwestern Europe) and underestimate it by up to 30% (e.g. in the Mediterranean) [22]. Therefore, we use a dataset that has been specifically bias corrected for Sweden [23,24]. The authors generated time series of future wind power production for 23 scenarios with different shares of onshore and offshore wind, different spatial distributions between Northern and Southern Sweden, and different capacity factors. The simulated annual power production ranges from 20 up to 70 TWh. For our analysis we use the time series of scenario C1 and D1 [23] (details on the validation can be found in Appendix A1). For the Wind scenario we used scenario D1 with an annual wind power generation of 70 TWh (whereof 20 TWh is new offshore generation). C1 assumes an annual wind power generation of 50 TWh (whereof 13 TWh is new offshore generation), which we scaled to 55 TWh assuming the same spatial configuration, for the Wind+PV scenario.

EMHIREs aims at reproducing wind and **solar power** time series at both national and regional levels within Europe using a homogeneous methodology. However, on a country level it is possible to achieve higher correlation values and a better representation of extreme ramping events by the use of additional correction factors [21]. For Sweden, EMHIREs provides hourly time series of PV capacity factors per bidding area (a detailed description of the Swedish bidding areas can be found in Appendix A2). We assume that no considerable PV generation capacities are installed in the most northern of the four Swedish bidding areas (SE1). In total, a PV capacity of 16.9 GW is needed to provide 14.9 TWh of electricity at mean capacity factors ranging from 9.70 % (SE2) to 10.7% (SE3) (Wind+PV scenario). Between bidding area SE2, SE3 and SE4 we distribute the solar generation capacities according to the electricity demand in the region. Therefore, the majority of the PV capacity (11.6 GW or 68.6%) is assumed to be installed in bidding area SE3.

### 2.3 Simulated load time series

For the simulation of hourly loads (electricity demand) of the entire 29-year period (1986-2014) we apply a statistical model that uses reanalysis temperature data and gridded population raster data to calculate the population weighted mean temperature, and historical load data of the Swedish transmission system operator (TSO) Svenska Kraftnät, to fit and validate the model.

Modern Era Retrospective-Analysis for Research and Applications (MERRA) reanalysis [6,25] provides consistent hourly temperature time series from 1979 up to now. It offers a spatial resolution of 0.66-degree longitude by 0.5-degree latitude, resulting in 267 grid cells for Sweden. In order to reduce the number of predictor variables for the regression model, we calculated a population weighted temperature index for each of the four Swedish bidding areas. For that purpose, we used the “Gridded Population of the World” (GPWv4) [26] data set. It provides population numbers consistent with national census at a 1 km grid resolution. We aggregated the population for each MERRA grid cell and then used the information to



calculate the mean temperature of all MERRA grid cells within one bidding area weighted by the population of the single MERRA grid cells. This ensures that the temperatures of more densely populated areas with higher electricity demand get a higher weight in the resulting mean temperature.

In Sweden the temperature sensitivity of load is mainly driven by heating while cooling is negligible under current conditions [27]. Therefore, the negative relationship between temperature and load can be observed for almost the entire temperature range. To estimate the response function of hourly load to temperature, we estimate a linear regression model for each of the four Swedish bidding areas. Besides temperature, hourly load (load) is affected by calendar effects as hourly, weekday our seasonal patterns [28–31]. The effect of the hour of the day, weekdays, and public holidays is modelled with dummy variables and seasonal cycles are modelled using Fourier series. The complete estimating equation is given by:

$$load(h) = \sum_{i=1}^3 \beta_i \tau_{i,h} + \sum_{j=4}^{27} \beta_j \delta_j^{hod} + \sum_{k=28}^{34} \beta_k \delta_k^{dow} + \beta_{35} \delta^{hol} + \beta_{36} * \cos \frac{p\pi h}{8760} + \beta_{37} * \sin \frac{p\pi h}{8760} \quad (1)$$

where  $\tau_i$  includes the mean weighted temperature of the current hour and the lagged temperature of the last hour and 24 hours ago.  $\delta_j^{hod}$  and  $\delta_k^{dow}$  are dummy variables for the hour of the day and the day of the week and  $\delta^{hol}$  is a dummy variable that covers the effect of public holidays.  $\beta_{36}$  and  $\beta_{37}$  are the amplitude coefficients that describe the two cycles within a year ( $p = 2$ ) of the Fourier series, while  $h$  is hour of the year [31].

For fitting the model, respectively choosing the values of  $\beta_{1-36}$ , we applied linear regression, i.e. we minimized squared errors, using historic data from 2010-2016 [32]. The prediction performance was evaluated using data for the years 2007- 2009 (see Appendix A3).

#### 2.4 Hydro and thermal power simulation model

We have developed a linear program that minimizes the residual load balancing demand. The main inputs for the model are hourly time series of the simulated natural river runoff (a detailed description how we simulated hydro power generation is given in Appendix A4), load, and wind and PV generation. The model is solved for 29 years with varying meteorological conditions and initial hydro reservoir levels that are determined from the operation in the year before.

The objective function aims to minimize the sum of the overall balancing demand given by the sum of hydro and thermal power generation plus potential loss of load events. We have designed the model to provide the maximum amount of balancing energy from hydropower and to use thermal power only when hydropower can not provide enough energy. Therefore, we use weighting factors to prioritize hydro generation and spilling (factor 1) over thermal (factor 2) and loss of load (factor 10).

$$\min net\_load\_balancing_{year} = \sum_h (hydro_h + spill_h + thermal_h * 2 + loss\_of\_load_h * 10), \forall year \quad (2)$$

This prioritization has an economic interpretation, as in general, variable costs (loss of load) > costs (thermal generation) > costs (hydropower generation). In Appendix A5 we show that the



results of the optimization model are insensitive to the choice of weights, as long as the order of weighting factors is maintained. The first constraint ensures that residual load (= Load- VRE generation) equals the sum of hydro and thermal power generation plus potential loss of load events at every hour. Negative residual load events (i.e. when VRE generation exceeds load) are assumed to be balanced by curtailments or exports with no additional cost.

$$net\_load_h = hydro_h + thermal_h + loss\_of\_load_h - curtailment_h, \forall h \quad (3)$$

Curtailment is limited by the sum of VRE and nuclear generation at each hour. It is necessary to include nuclear generation here to keep the model feasible in the Reference scenario. However, it has no impact on the fully renewable energy scenarios.

$$curtailment_h \leq VRE_h + nuclear_h, \forall h \quad (4)$$

Our goal was to provide a simple model that captures the overall flexibility of hydro and thermal power plants, rather than a detailed dispatch model at power plant level. Therefore, we aggregated the generation capacities to one plant per generation technology (i.e. one hydropower plant with one reservoir and one thermal power plant). In 2014, the installed capacities amounted to 16.2 GW for hydropower (cap\_hydro) and 8.4 GW for thermal power (cap\_thermal) [16]. Our approach to aggregate the generation capacities of all plants is not able to capture operational restrictions of single plants. Instead we derive operational restrictions (i.e. maximum capacity factors) from observed operational data between 2007 and 2014 [32]. Within this period, the maximum hydropower generation was 13.7 GW or 85 % (cfHydro) of the installed capacity and 6.6 GW or 79 % for thermal power plants (cfThermal).

$$hydro_h \leq capHydro * cfHydro \quad \forall h \quad (5)$$

$$thermal_h \leq capThermal * cfThermal \quad \forall h \quad (6)$$

Additionally, we implemented a minimum flow constraint to account for restriction due to water legislation of 1.5 GWh (minFlow). Maximum flow is limited by the historic maximum power generation and the maximum hourly water spill (spill\_h) that is allowed is one 1 GWh (max\_spill).

$$hydro_h + spill_h \geq minFlow, \forall h \quad (7)$$

$$spill_h \leq maxSpill, \forall h \quad (8)$$

Most thermal power plants are CHP (combined heat and power) plants that have to supply heat for district heating networks. Therefore, we have assumed that the hourly minimum generation for each month has to be higher than the average hourly generation of the same month with the lowest generation in the period from 2007 to 2014. Thus, the hourly minimum thermal generation ranges from 197 MW in July up to 1470 MW in January.

Hourly ramps for both thermal and hydropower plants have been restricted by the maximum observed ramps in the past (i.e. maxRampHydro = 4.0 GW and maxRampThermal = 1.5 GW).

$$|hydro_h - hydro_{h-1}| \leq maxRampHydro, \quad \forall h \quad (9)$$

$$|thermal_h - thermal_{h-1}| \leq maxRampThermal, \quad \forall h \quad (10)$$

The following equation ensures that the reservoir level at each hour equals the reservoir level of the previous hour plus inflows minus hydropower generation and spilled water.

$$res\_level_h = res\_level_{h-1} + inflow_h - hydro_h - spill_h, \forall h \quad (11)$$

Furthermore, the reservoir level has to be kept between the minimum (5 %) and maximum (98 %) observed storage levels of the total reservoir capacity (33.7 GWh) for all hours [33].

$$res\_level_h > reservoirCap * 0.05, \forall h \quad (12)$$

$$res\_level_h < reservoirCap * 0.98, \forall h \quad (13)$$

To ensure operational flexibility for the next year, the reservoir has to be at least half full at the end of the year. This corresponds to the historically observed minimum reservoir levels at the end of the year from 1960 to 2015.

$$res\_level_h > reservoirCap * 0.50, h = 8760 \quad (14)$$

The reservoir level for the first hour of the year is set to reservoir level at the end of the previous year, except for the first simulation year, where we assume that the reservoir is filled to 70 %, which is the long-term mean at the first week of the year.

The resulting hourly time series of hydro- and thermal power generation, loss of load and curtailment are used to assess the occurrence and frequency of extreme residual load events (potential loss of load events).

### 3 Results

In the first part of the results section we analyse seasonal and interannual variations of residual load and hydropower generation to show how different mixes are affected by climate variability. In the second section we focus on aspects of fully renewable power systems that affect the short-term flexibility of the power system. These include measures to balance hourly and daily fluctuations of residual load such as the change in extreme ramping events and the need for backup, storage, and transmission capacities.

#### 3.1 Seasonal and interannual variability of VRE generation and load

Wind power generation in Sweden shows no clear diurnal pattern, but a favourable seasonal profile with slightly higher production during the winter when electricity demand is higher. PV on the other side has an unfavourable seasonal profile with high production during summer and depending on the generation site, low to zero generation in winter. The diurnal profile of PV, however, matches load quite well, with peak generation during midday and no generation during night.

Figure 1 shows the simulated seasonal patterns of electricity demand and VRE generation. The influence of heating and lighting requirements leads to higher load during winter and low demand during summer with minima during the holiday season in July and August. The daily mean hourly load ranges from 10.9 GW on a typical day in July up to 18.5 GW in January. The comparison of daily mean hourly loads over the 29 year period (shaded area in Figure 1) reveals considerable variability, especially during winter. Daily mean hourly loads in the simulated time series in January range from 14.3 GW on the mildest winter days up to 26.9

GW for the coldest days in January 1987, which was the coldest month between 1980 and 2016. The variation of summer loads is significantly lower, as electricity demand for cooling is a minor issue in Sweden. They range from 8.26 to 15.4 GW between May and September. The hourly maximum loads range from up to 29.1 GW in January to a maximum of 15.1 GW in July.

Compared to electricity demand, PV generation shows a clear anticyclic pattern, with 80 % of the annual solar PV output generated in spring and summer. On sunny summer days, the daily mean PV generation reaches 5.0 GW. On cloudy days though, generation could be as low as 0.6 GW, despite the spatial distribution of PV capacities across Sweden. From November to February, when load is highest, the contribution of PV generation to the electricity supply is negligible, with daily mean generation not exceeding 0.8 GW. Mean capacity factors for PV thus range from about 18 % in summer to below 5 % in February and November, and below 2 % in January and December.

During this time of the year a fully renewable energy system, therefore, would have to rely on other renewable energy generation capacities. Wind generation follows a similar seasonal pattern as load, with slightly higher production during autumn and winter. In the Wind scenario, mean hourly generation ranges from 6 GW in the summer to 9.6 GW in the winter months. This corresponds to mean capacity factors of about 50 % in the winter months, from December to February, and about 30 to 33 % in the summer months, from June to August. Low wind generation events with a daily mean hourly generation of less than 1.2 GW can occur during the whole year. However, in winter, such events are very rare and occur on only 13 days within the full 29-year simulation period (light blue shaded area in Figure 1).

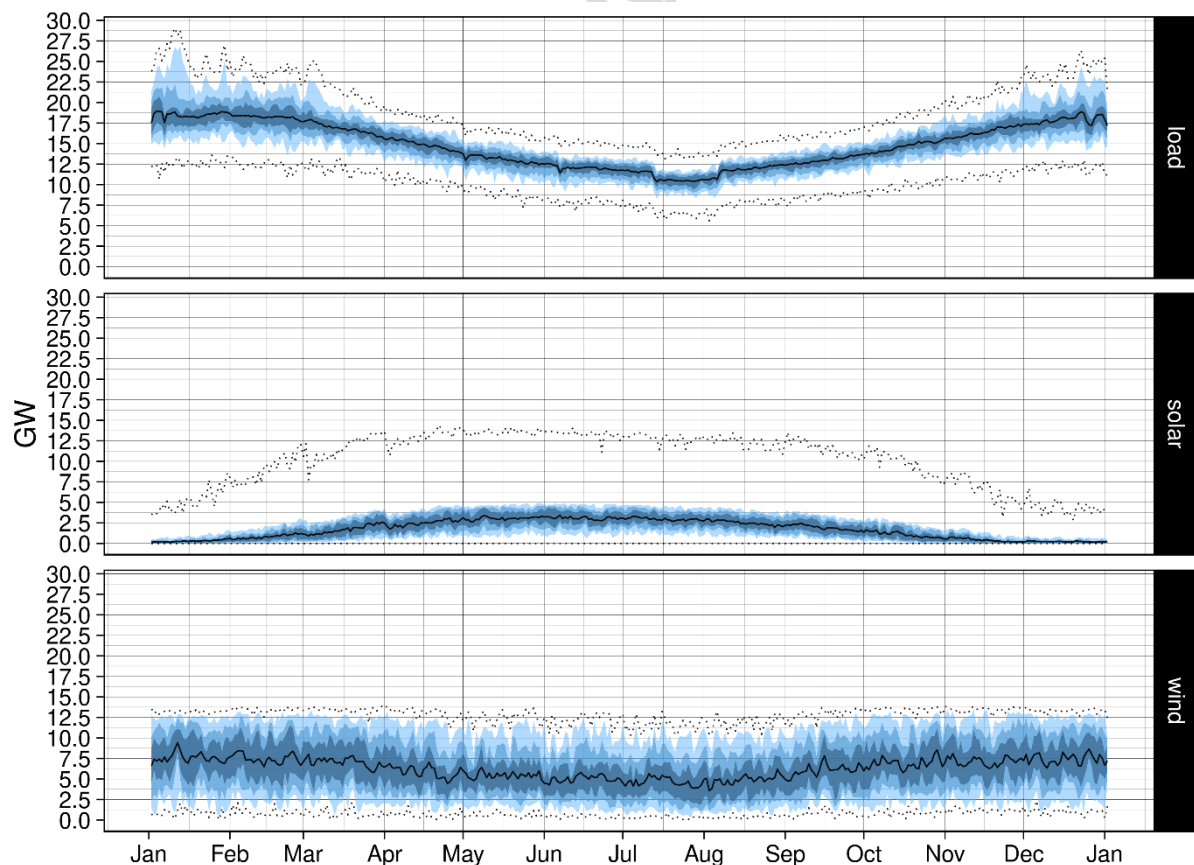


Figure 1: Interannual and seasonal variation of simulated electricity demand (load), solar PV and wind generation from 1986

to 2014 in the Wind+PV scenario. The black line shows the daily mean values over 29 years of simulated temperature dependent load and generation. The shaded areas indicate the observed variation of daily mean values in the simulated time series: minimum and maximum values in light blue, 10th to 90th percentile in blue and 25th to 75th percentile in dark blue. The dotted lines show the hourly minimum and maximum load and generation for each day.

The annual electricity demand varies between 125 and 136 TWh in all simulated scenarios (Figure 2). This corresponds to maximum deviations of 4.62 % from the long term mean of 130 TWh. Annual capacity factors vary between 29.5 and 34.5 % for wind energy, and between 6.87 and 8.58 % for PV. In the Wind+PV scenario, annual wind energy generation thus varies between 50.5 and 59.5 TWh, and PV generation between 13.3 and 16.5 TWh. Deviations from the long-term mean annual generation range from -8.40 to +8.00 % for wind generation and from -11.6 to +10.0 % for PV generation. Interannual variability of VRE generation is thus not higher than the historic variability of hydro, which experienced deviations of -17.1 to +12.0 %, between 2007 and 2016.

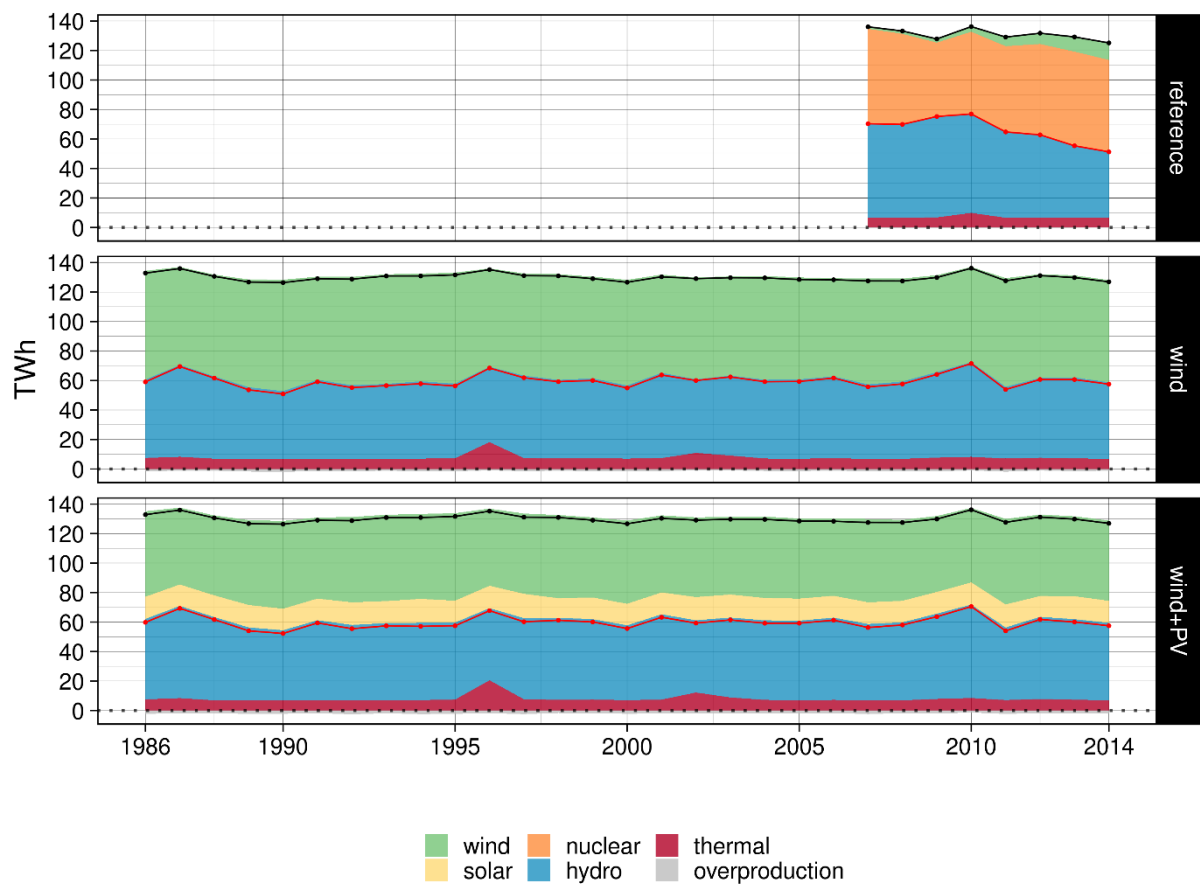


Figure 2: Simulated annual load (black line), residual load (red line) and generation by source (nuclear, thermal, hydro, wind and solar PV) for weather years 1986 to 2014 (the reference scenario relies on historic data from 2007 to 2014). Note that the simulated time series assume constant capacities as given in our scenarios over all years and thus do not reflect historic generation but the effect of interannual climatic variability on VRE generation and load.

The combined effects of load and VRE generation on residual load (=load - wind - solar - nuclear) are shown in Figure 2. From 2007 to 2014, the actual annual residual load (reference scenario) varied between 51.3 TWh in 2014 and 77.0 TWh in 2010. Over the complete 29-year period from 1986 to 2014, we observe similar minimum residual loads in the fully renewable power scenarios (Wind and Wind+PV) of 50.9 and 52.3 TWh per year. Annual maximum residual loads are lower with 71.5 and 70.5 TWh in the Wind and Wind+PV scenario,

respectively. Annual power generation is 7.61 and 8.08 TWh higher than the annual load in the Wind and Wind+PV scenario, respectively. In years with above average hydropower generation (e.g. in the year 2000) overproduction can reach up to 2.4 TWh. In the reference scenario, from 2011 to 2016 Swedish net electricity exports varied between 7.23 and 22.6 TWh[32].

### 3.2 Long-term correlations of VRE generation and load

So far we have shown that electricity demand and wind generation are higher during the winter period while PV produces about 80% of its output during the summer months. However, to better understand the risk of extreme residual load events it is crucial to assess interannual variations and to determine the long-term correlations of load, hydropower, and VRE generation. Therefore, we analyse the long-term correlations of monthly load, VRE generation and natural river runoff (Figure 3). As the time series with 29 years of simulated data is still relatively short to get meaningful results for the correlations of annual data, we compare deseasonalized monthly load and generation to assess if it is more likely that a month with above average electricity demand is associated with low or high VRE generation in the same period. Of specific interest for our analysis is the relationship between wind power output and electricity demand (load) during the winter month. During this time the probability of loss of load events is highest due to the higher electricity demand and the negligible PV generation.

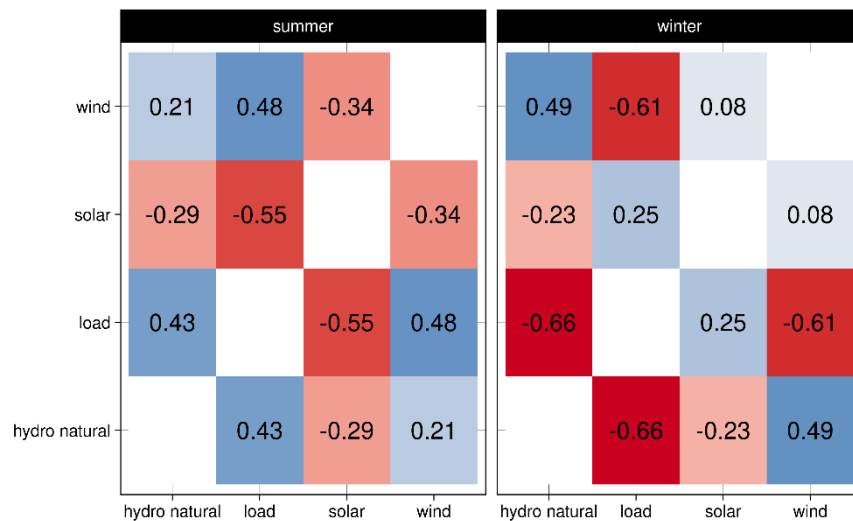


Figure 3: Correlation matrix (red: negative, blue positive) of deseasonalized monthly load, solar, wind and simulated hydro generation for the summer (June, July and August) and winter months (December, January and February)

In the context of extreme residual load events, the negative correlations of -0.61 between wind and load and -0.66 between natural river runoff and load during the winter months, are particularly interesting. This means that high shares of wind energy might considerably increase the pressure on the power system's balancing capacities, as it is likely that periods of high electricity demand coincide with periods of low wind power output. Contrarily, PV generation shows moderately positive correlations during winter ( $r = 0.25$ ) and negative correlations during summer ( $r = -0.55$ ). Considering the small overall PV generation during winter the potential to balance peak loads during winter is limited, while the negative

correlation during summer is likely to result in negative residual loads (overproduction) and the need to curtail VRE generation.

### 3.3 Variability and hourly ramps of residual load

In the previous section, we have shown that load as well as VRE and hydro generation fluctuate considerably from year to year and that severe winters with above average electricity demand are more likely to coincide with relatively low wind generation and river runoff. In this section, we explore the resulting residual load variations in more detail, to assess the impact on the balancing capabilities of the power system. We define residual load as load – wind – PV – nuclear generation. This thus corresponds to the amount of electricity that has to be met by hydro and thermal power plants, as well as imports and exports.

The mean monthly residual loads in the fully renewable scenarios are on average slightly lower than the ones in the current power system (see Table 2). Replacing nuclear power capacities by wind (Wind scenario) lowers the variability of monthly residual loads, while adding PV capacities increases the standard deviation due to the strong seasonal pattern of PV generation.

*Table 2: Comparison of monthly residual loads (TWh/month) in the three scenarios*

Scenario	Mean	Standard deviation	Min	Max
Reference	5.3	1.6	1.8	10.1
Wind	5.0	1.5	2.2	10.2
Wind+PV	5.0	2.1	1.5	11.2

From 2007 to 2014 (reference scenario), the mean hourly residual load was 7.5 GW (with a standard deviation of 3.1 GW) (see Figure 4). The minimum and maximum hourly residual load was -1.1 GW and 18.6 GW, respectively. In 3.5 % of the time (on average 306 hours per year) residual load exceeded the maximum hydropower generation capacity (red dotted line in figure), while negative residual loads occurred in only 0.2 % of the time (on average 17 hours per year). The fully renewable scenarios both show a significant increase in more extreme residual load events. The frequency of negative residual loads increases to 6.5 % and 8.0 % of the time in the Wind scenario and the Wind+PV scenario, respectively. Hours with a higher residual load than maximum hydro generation increases to 7.5 % and 9.0 % of all hours, in the Wind and Wind+PV scenario, respectively.

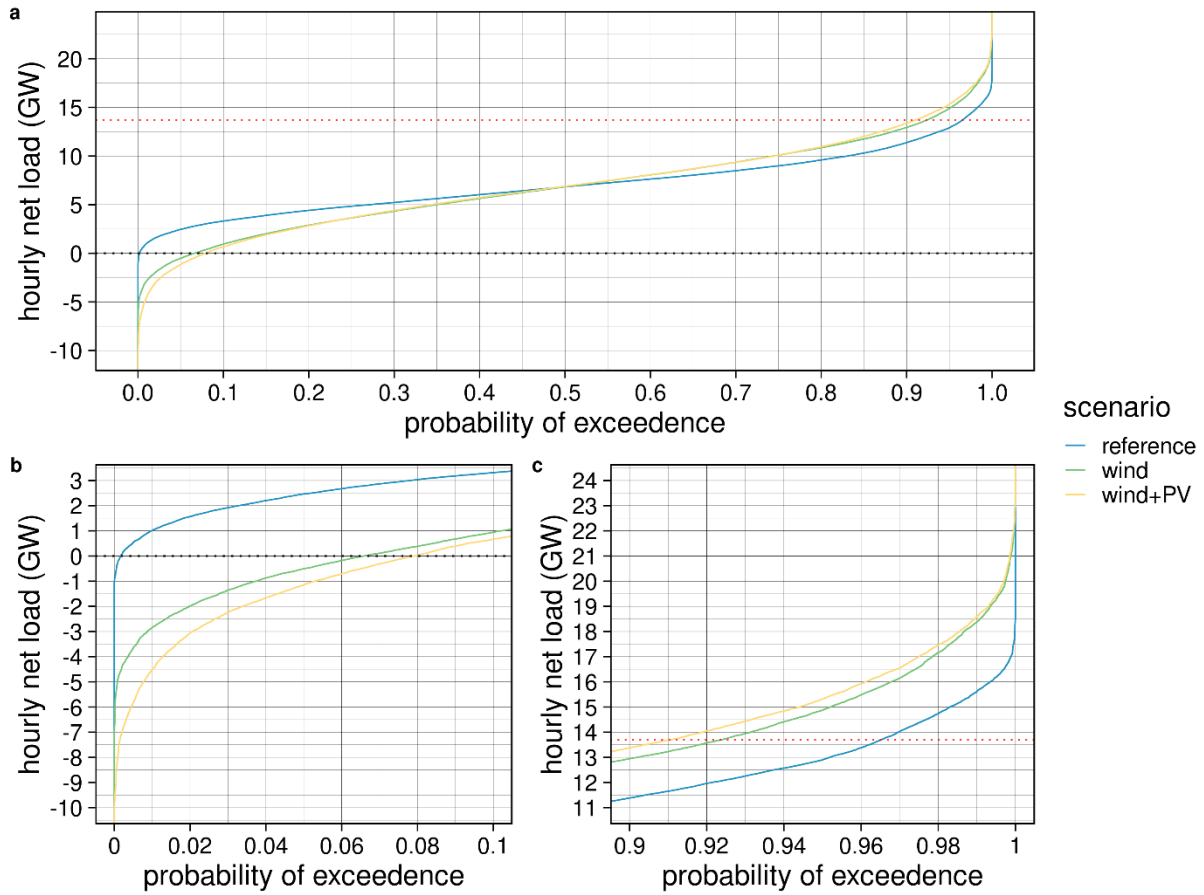


Figure 4: Distribution of hourly residual loads in the reference and the fully renewable scenarios. We define residual load here as load – wind – PV – nuclear. The red dotted line shows the maximum observed hydropower generation between 2007 and 2014. Above: full distribution. Below: Lower and upper end of distribution.

With the transition to a fully renewable power system, not only high and low hourly residual loads increase substantially, but also the frequency and magnitude of hourly ramps (Figure 5). In the past (Reference scenario) hourly residual load ramps ranged from -1.6 GW (for ramping down) to 2.3 GW (for ramping up). These fluctuations could be easily balanced by hydropower with hourly ramping rates ranging from -2.6 to 3.8 GW (observed historical ramps, orange in figure). For thermal power plants, historical ramps ranged from -2.2 to 0.9 GW and for imports and exports from -1.7 to 1.9 GW. However, the combined ramps (total) of hydro, thermal and imports and exports were significantly lower than the hydropower ramps. This demonstrates that in the past hydropower ramps were highest when the ramps of imports and exports were the lowest and vice versa. Thus, ramping up of hydropower generation was highest when imports decreased, or exports increased, substantially from one hour to another.

In the fully renewable power scenarios, the demand to balance hourly fluctuations increases significantly. In the Wind scenario the ramps range from -3.60 to 3.91 GW. This exceeds the observed total ramping rates of balancing capacities in 0.304 % of the time or on average 26.6 hours per year. The Wind+PV scenario produces far more extreme ramping rates ranging from -11.1 to 10.8 GW, which is three to four times more than the observed maximum historic ramping rates of hydropower. It would exceed the observed total ramping rates of balancing capacities in 3.86 % or on average 338 hours per year. In this case also the observed historic



hydropower ramps would not be able to balance 0.619 % of the ramping down events and 0.0856 % of the ramping up events.

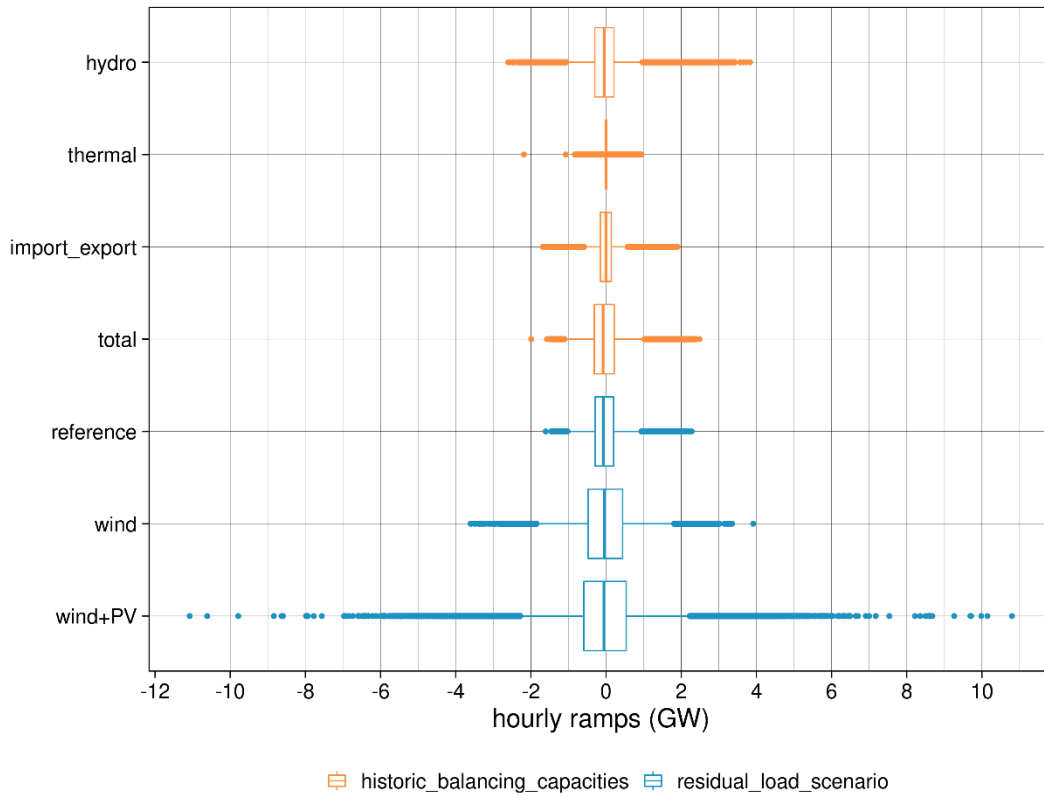


Figure 5: Hourly residual load ramps (blue) in the three scenarios (Reference, Wind and Wind+PV) compared with historically observed ramps of balancing capacities (orange) (hydro and thermal power plants, as well as imports and exports). The “total” ramp boxplot shows the observed combined hourly ramps of all balancing capacities.

### 3.4 Extreme residual load events

In this section we assess the frequency, magnitude and duration of extreme residual load events in a fully renewable power system for Sweden. As extreme residual load events we define events that exceed the balancing capacity of the current hydro and thermal power capacities. The main focus of our analysis are positive residual load events, thus events where the load exceeds the generation capacities of the hydro and thermal power plants. For those events, a fully renewable power system would need additional backup capacities to avoid loss of load events. Besides that, integrating large shares of VRE substantially increases the occurrence of negative residual loads, where the generation of wind and PV is higher than the electricity demand. These events can be handled more easily by the curtailment of VRE generation, but the need to curtail large shares of VRE generation still affects their overall generation costs and thus the feasibility of a fully renewable power system. Therefore, we will highlight the occurrence of negative residual load events in the second part of this section.

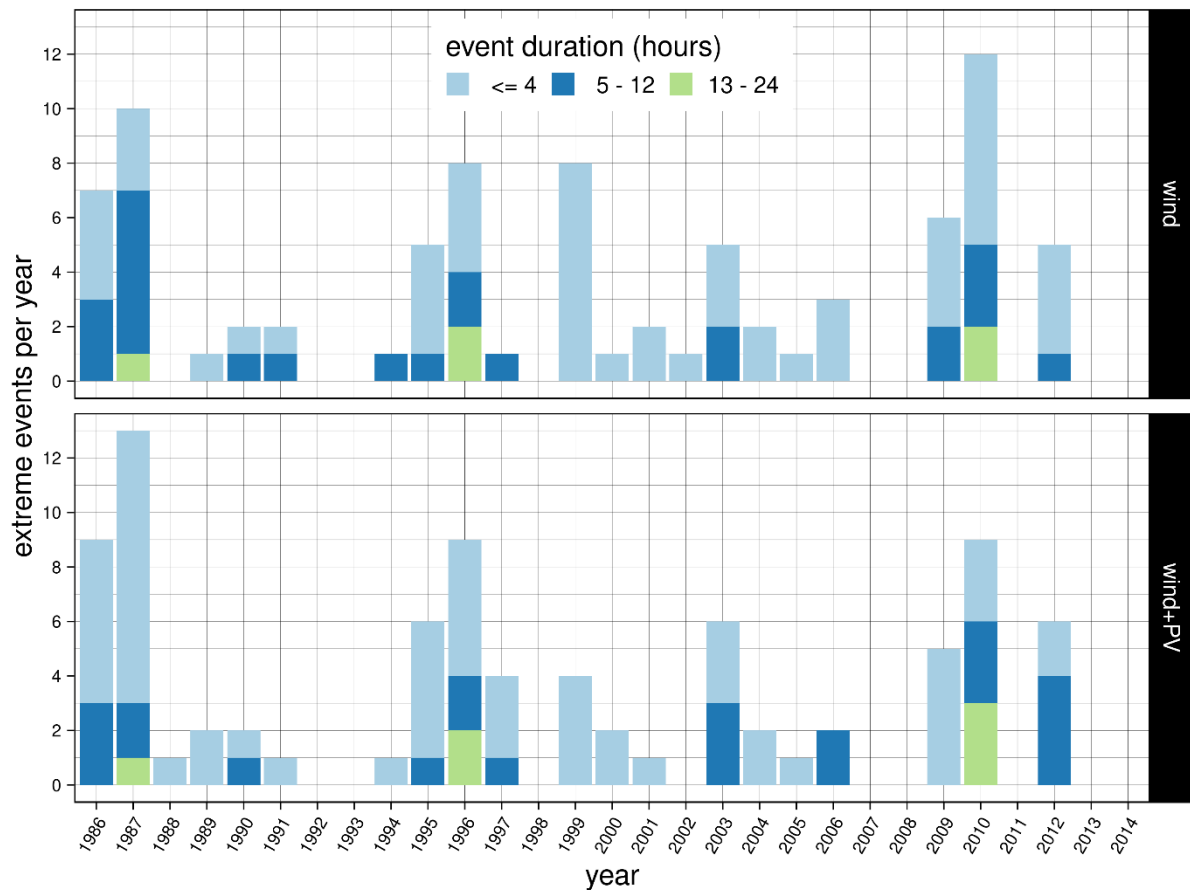


Figure 6: Number of extreme residual load events in the Wind and Wind+PV scenarios that exceed the balancing capacity of current hydro and thermal power plants. Note that the simulated time series assume constant capacities as given in our scenarios over all years and thus do not reflect historic generation but the effect of interannual climatic variability on VRE generation and load.

Over the complete 29-year period, we observe 83 and 86 extreme residual load events in the Wind and Wind+PV scenario, respectively (Figure 6). The occurrence of extreme events shows considerable interannual variations. In nine out of the 29 years, the occurring residual loads can be balanced by the current hydro and thermal backup capacities in both the Wind and the Wind+PV scenario, and we therefore observe no extreme residual load events. The climatic conditions of 1987, 1996, and 2010 result in the highest number of extreme residual load events, with eight or more events, several of which are long duration events, per year in both scenarios. In total about 36 % of all extreme residual load events over the 29-year period occur within these three years.

On average our simulation results show about three extreme residual load events per year. In total the simulated extreme residual load events sum up to 359 and 372 hours, respectively, with a lack of capacity in both scenarios. This corresponds to an average of about 13 hours per year. However, in the Wind scenario, only in one third of those hours the lack of balancing capacities exceeds 1 GW and only in about 12 % more than 2 GW of additional balancing capacities are needed. In the Wind+PV scenario the additional balancing needs are slightly higher with 39 % of all hours above 1 GW and 13 % above 2 GW. Overall, both fully renewable power scenarios result in relatively few events with a lack of capacity of more than 2 GW, when seen over whole 29-year period; amounting to 11 events for the Wind scenario, and 9

for the Wind+PV scenario, respectively. The highest lack of balancing capacity reaches 4.8 GW in both scenarios.

The Wind scenario results in six events lasting longer than 12 hours with a maximum duration of 15 hours, while the Wind+PV scenario shows five events with a maximum duration of 18 hours. Events between 5 and 12 hours are more frequent in the Wind scenario, with 24 compared to 22 events in the Wind+PV scenario. Shorter events that last less than five hours are the ones with lower additional capacity demands (Figure 7). The additional balancing capacity need during those events is mostly below 1 GW. Contrarily, in events that last longer than 12 hours, the lack of capacity ranges from 2 up to 4.4 GW.

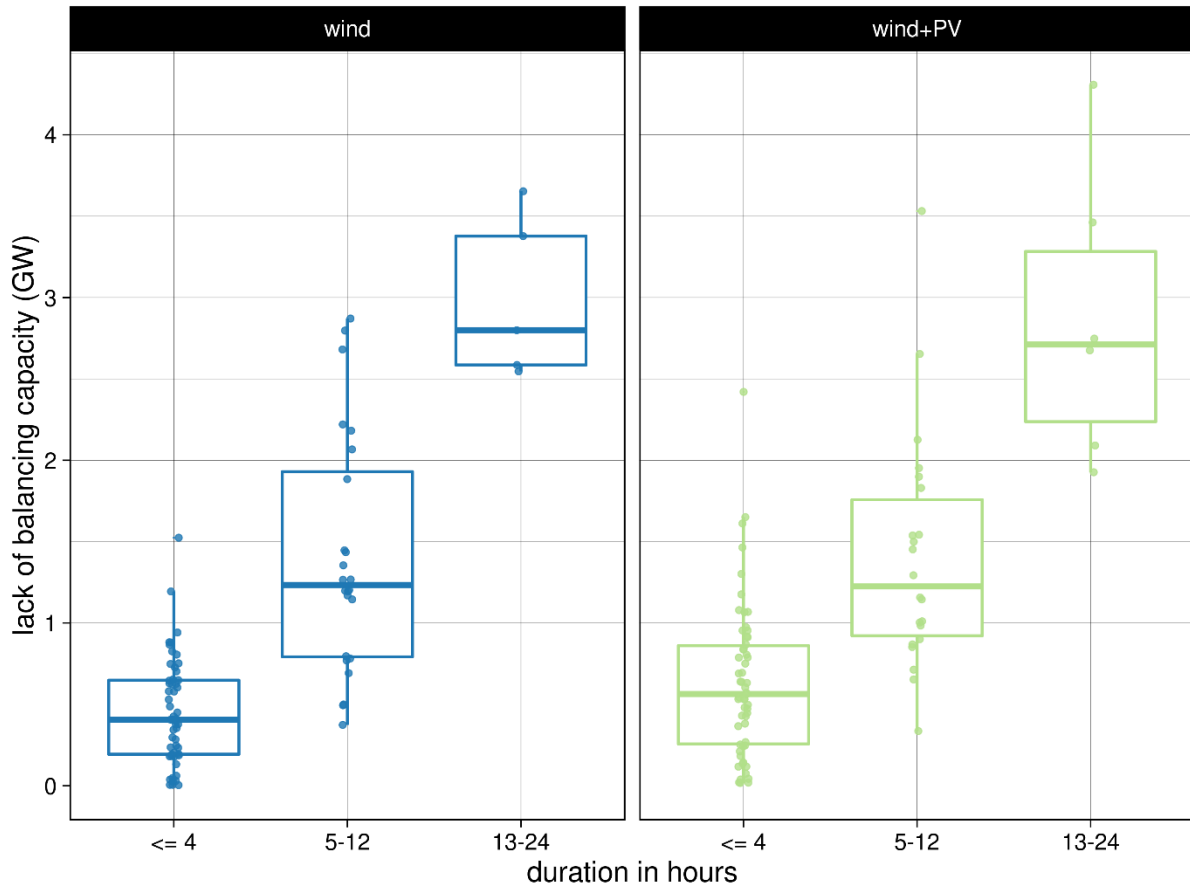


Figure 7: Lack of balancing capacities in the Wind and Wind+PV scenarios, grouped by the duration of the extreme residual load events

The hourly load and generation profiles for the second week of 1987 - the period with the highest and longest net load event - in both scenarios are shown in Figure 8. In both scenarios the combination of high load (peak at 27 GW) and for the season extremely low wind generation of below 2 GW on 7 January 1987 results in residual loads that can not be balanced even by assuming maximum hydro and thermal generation. In the Wind+PV scenario, PV generation is able to lower the loss of load for about 4 hours around midday but is too low with 1.8 to 2.9 GW to cover up for the extremely low wind generation. At the same time, the lower installed wind capacity in the Wind+PV scenario leads to an about 0.9 GW higher lack of capacity in the late afternoon hours of the same day, with 4.4 GW compared to 3.5 GW in the Wind scenario. In total, additional backup generation, imports, or storage of 39.4 and 41.3

GWh within 14 and 18 hours are required in the Wind and the Wind+PV scenario, respectively, to avoid a loss of load event.

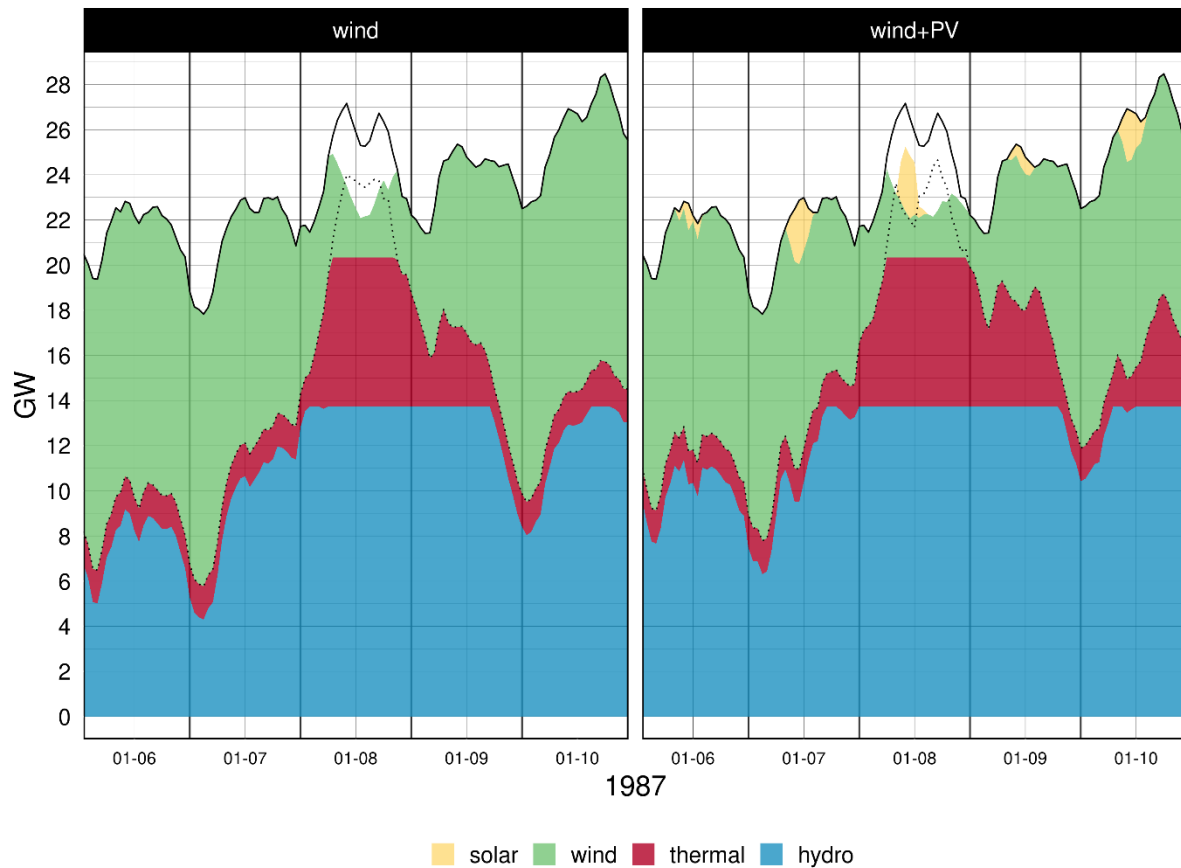


Figure 8: Hourly load (black line), residual load (black dotted line) and generation capacities (solar, wind, thermal and hydro) for the simulated week using weather data from 1987 with the highest and longest extreme residual load event within the complete 29 year period.

## 4 Discussion

We found that switching to a fully renewable power system with VRE shares of about 50 % would result in 83 and 86 extreme residual load events in the Wind and Wind+PV scenario, respectively, over the complete 29-year simulation period, if no additional flexibility options are made available in the Swedish power system. On average those events last 4.3 hours with a lack of balancing capacity of around 0.6 GW. One third of the events needs balancing capacities of more than 1 GW and six and five events, respectively, last longer than 12 hours. This highlights the challenges that even highly flexible power systems as the Swedish one, with its high share of hydropower and reservoirs that can store up to quarter of the annual electricity demand, will face when accommodating VRE shares of about 50 %.

In general, our assessment follows a conservative approach, i.e. real flexibility should be higher in the system, as imports and exports are not regarded in the model and only historical system flexibility is considered. Also, the temperature dependent load time series slightly overestimate high load events during winter (see Appendix A3). Our modelling approach of simulating hydro power with one large reservoir and power plant, provides time series of hydro power generation that are in line with maximum historic generation and hourly ramping rates. Scenarios with high VRE shares result in an unprecedented variability of hydro power

generation within days and from day to another. More detailed regional analyses need to verify, whether those new operational schedules can be met by individual reservoirs' and power plants' limitations as well as environmental regulations for single rivers. Accounting for those limitations could regionally reduce the ability of hydropower to provide system flexibility in extreme climatic situations, i.e. a hot and dry season followed by a cold winter with low wind. Our optimization approach prioritizes hydro over thermal power generation. Thus, hydro power plants reach their maximum generation capacities more often, while at the same time thermal power generation tends to be lower than historically observed. Therefore, there is still flexibility in the system to switch between hydro and thermal power generation that is not reflected in the results.

Another flexibility restriction of the real power system, which is not considered here, is the transmission system. Further studies would have to assess the limitations imposed by transmission limits. Also, we only assess extreme events on the demand side caused by climate. Extreme events caused by other factors (such as e.g. outages of power plants) are not assessed.

In our reference scenario with about 45 % of the electricity coming from nuclear power plants, the maximum hourly residual load reaches about 19 GW, which is equivalent to the combined peak generation from hydro and thermal power between 2007 and 2014. Replacing base load nuclear power capacities by VRE in the two fully renewable scenarios increases the simulated maximum hourly residual loads by about 4.0 GW to about 23 GW in both scenarios. The variability of wind and PV generation also increases the maximum hourly ramps up to 3.9 GW in the Wind scenario, and up to 11 GW in the Wind+PV scenario. The hourly ramps in the two fully renewable scenarios exceed the ramping capacities of the current system on average 26 and 338 times per year, respectively.

Seasonal and diurnal variations of VRE generation and load have previously been studied on different scales [34–36] and are generally well understood. Our results demonstrate that also extreme residual load events follow clear patterns. Typically, they occur during daytime on weekdays in winter, as those are the times with peak demand when low VRE generation cannot be balanced by hydro and thermal power generation. Our results further show that events that cannot be balanced with current balancing capacities could last up to 18 hours. During the night, when electricity demand is generally lower, also events related to extremely low VRE generation can be balanced more easily. Our analysis also confirms results that extreme events (at least in Northern Europe) are clearly a winter phenomenon [36–38], with all residual load events occurring between December and March.

Our results provide valuable information on the frequency, duration and magnitude of extreme residual load events (potential loss of load events). However, further research is needed to assess the implications of these extreme events on the cost optimal design of flexibility and backup options. Possible options range from adding hydropower and thermal biomass balancing capacities or investing into storage and demand response technologies to balance short-term peaks of residual load.

Current environmental regulations limit the potential for new hydropower plants. However, hydropower generation could be expanded through efficiency improvements of current

hydropower plants by 2 to 4 TWh annually, and new hydro plants on non regulated water courses could provide additional 6 TWh [16]. If only half of this potential is realized, about 1.5 GW of additional capacity would be available for balancing extreme residual load events. Our results highlight that wind power expansion intensifies extreme residual load events during winter. Biomass CHPs represent a viable substitute for this period as heat demand is highest on cold winter days. The fact that only a few hours per year require additional balancing capacity makes it questionable though, whether new biomass capacities can provide a cost optimal backup solution. Another option would be to foster demand response management. Measures to increase demand flexibility of Swedish industry and households could provide 3 to 5 GW for short extreme residual load events of up to three hours [39]. Measures that address reducing or shifting peak electricity demand for heating are of particular interest, as it can amount to 7 GW in a normal and up to 8 GW in a severe winter [39]. Demand response seems a reasonable option, considering the low frequency of extreme net load events that last longer than 4 hours (8 and 8.5 hours per year in the Wind+PV and the Wind scenario, respectively), as well as the fact that in the majority of extreme residual load events (66 % in the Wind scenario and 63 % in the Wind+PV scenario) the lack of balancing capacity is below 1 GW.

## 5 Conclusions

Our results build on a modelling framework that uses long-term simulated time series of hourly VRE generation, river-runoff and load, combined with an optimization model that incorporates operational restrictions of hydro and thermal power plants (i.e. maximum generation and ramping capacities as well as reservoir management). This approach allows us to study the interannual variations of residual load and the impact of climatic extreme on the flexibility demands of the power system to guarantee security of supply.

The importance of using long-term time series of VRE generation and load has been stressed by several authors before, as interannual climate variability affects VRE generation and load [38,40], but is also responsible for large fluctuations of generation costs and CO<sub>2</sub> emissions [5,41]. Over the complete 29-year period that uses climatic data from 1986 to 2014, simulated annual loads deviate up to 4 % from the long term mean of 130 TWh. Renewable energy generation shows much greater interannual variability with deviations from the mean of up to 8, 12 and 18 % for wind, PV and hydropower generation, respectively. Annual residual loads range from 50.9 up to 71.5 TWh.

These results highlight the importance of using long-term time series of VRE generation and load for assessing the impact of extreme climatic events on power systems with high shares of VRE, as in about one third of the simulation years we do not observe any extreme residual events, while fully 37 % of the events occur within the three years with the most extreme climatic conditions (1987, 1996, and 2010). The strong impact of climate is highlighted by the fact that temperatures during extreme residual load events within these three years were 5 to 15°C below long term average. Increasing temperatures due to climate change may cause a decrease in the probability of these events. However, they still cannot be ruled out in the future.

Simulated time series do not perfectly reflect fluctuations of load and VRE generation and may, as shown in the appendix, slightly overestimate the occurrence of extreme residual load events. However, relying on shorter periods of observed data may lead to even more problematic results, as it is unlikely that time series of only one or a few years capture the most extreme climatic events.

The key insight from our analysis is that highly flexible power systems as the Swedish one are able to accommodate VRE shares of up to 50 % in a fully renewable power system and to balance the resulting VRE fluctuations on various time scales ranging from interannual and seasonal to hourly. However, extreme climatic events (i.e. cold winter days with extremely low wind generation) that occur for only some hours per year still exceed the balancing capacity of the current power system. The key question that future research needs to address is, whether investments in new backup or storage capacities to balance those very rare residual load events or measures to achieve higher demand flexibility can provide more cost efficient solutions.

### Acknowledgements

This research has been conducted within the project “Integrating renewable electricity systems with the biomass conversion sector: a focus on extreme meteorological events” financed by the Swedish Research Council Formas (dnr. 2016-20118). Bio4Energy is also gratefully acknowledged for financial support.



## 6 References

- [1] GEA. Global Energy Assessment - Toward a Sustainable Future. Cambridge University Press, Cambridge, UK and New York, NY, USA and the International Institute for Applied Systems Analysis, Laxenburg, Austria: 2012.
- [2] IRENA. Renewable Energy Statistics 2018. Abu Dhabi: The International Renewable Energy Agency; 2018.
- [3] IRENA. Renewable Energy Auctions: Analysing 2016. Abu Dhabi: The International Renewable Energy Agency; 2017.
- [4] Després J, Mima S, Kitous A, Criqui P, Hadjsaid N, Noirot I. Storage as a flexibility option in power systems with high shares of variable renewable energy sources: a POLES-based analysis. *Energy Econ* 2017;64:638–650. doi:10.1016/J.ENERCO.2016.03.006.
- [5] Zeyringer M, Price J, Fais B, Li P-H, Sharp E. Designing low-carbon power systems for Great Britain in 2050 that are robust to the spatiotemporal and inter-annual variability of weather. *Nat Energy* 2018;3:395–403. doi:10.1038/s41560-018-0128-x.
- [6] Molod A, Takacs L, Suarez M, Bacmeister J. Development of the GEOS-5 atmospheric general circulation model: evolution from MERRA to MERRA2. *Geosci Model Dev* 2015;8:1339–56. doi:10.5194/gmd-8-1339-2015.
- [7] Huber M, Dimkova D, Hamacher T. Integration of wind and solar power in Europe: Assessment of flexibility requirements. *Energy* 2014;69:236–46. doi:10.1016/j.energy.2014.02.109.
- [8] Olauson J, Ayob MN, Bergkvist M, Carpmann N, Castellucci V, Goude A, et al. Net load variability in Nordic countries with a highly or fully renewable power system. *Nat Energy* 2016;1:16175. doi:10.1038/nenergy.2016.175.
- [9] Rodriguez RA, Becker S, Greiner M. Cost-optimal design of a simplified, highly renewable pan-European electricity system. *Energy* 2015;83:658–68. doi:10.1016/j.energy.2015.02.066.
- [10] Schmidt J, Cancelli R, Pereira AO. The role of wind power and solar PV in reducing risks in the Brazilian hydro-thermal power system. *Energy* 2016;115:1748–57. doi:10.1016/j.energy.2016.03.059.
- [11] Brown TW, Bischof-Niemz T, Blok K, Breyer C, Lund H, Mathiesen BV. Response to ‘Burden of proof: A comprehensive review of the feasibility of 100% renewable-electricity systems.’ *Renew Sustain Energy Rev* 2018;92:834–47. doi:10.1016/j.rser.2018.04.113.
- [12] Després J, Mima S, Kitous A, Criqui P, Hadjsaid N, Noirot I. Storage as a flexibility option in power systems with high shares of variable renewable energy sources: a POLES-based analysis. *Energy Econ* 2017;64:638–50. doi:10.1016/j.eneco.2016.03.006.
- [13] Heide D, von Bremen L, Greiner M, Hoffmann C, Speckmann M, Bofinger S. Seasonal optimal mix of wind and solar power in a future, highly renewable Europe. *Renew Energy* 2010;35:2483–9. doi:10.1016/j.renene.2010.03.012.
- [14] Welsch M, Deane P, Howells M, Ó Gallachóir B, Rogan F, Bazilian M, et al. Incorporating flexibility requirements into long-term energy system models – A case study on high levels of renewable electricity penetration in Ireland. *Appl Energy* 2014;135:600–15. doi:10.1016/j.apenergy.2014.08.072.
- [15] Swedish Energy Agency. Energy in Sweden - Facts and Figures. 2018.
- [16] Byman K. Future Electricity Production in Sweden. Stockholm: The Royal Swedish Academy of Engineering Sciences (IVA); 2016.
- [17] Energikommisionen. Kraftsamling för framtidens energi. Stockholm: 2017.
- [18] Lund PD, Lindgren J, Mikkola J, Salpakari J. Review of energy system flexibility measures to enable high levels of variable renewable electricity. *Renew Sustain Energy Rev* 2015;45:785–807. doi:10.1016/j.rser.2015.01.057.

- [19] Lindström G, Pers C, Rosberg J, Strömqvist J, Arheimer B. Development and testing of the HYPE (Hydrological Predictions for the Environment) water quality model for different spatial scales. *Hydrol Res* 2010;41:295–319. doi:10.2166/nh.2010.007.
- [20] Strömqvist J, Arheimer B, Dahné J, Donnelly C, Lindström G. Water and nutrient predictions in ungauged basins: set-up and evaluation of a model at the national scale. *Hydrol Sci J* 2012;57:229–47. doi:10.1080/02626667.2011.637497.
- [21] Gonzalez Aparicio I, Zucker A, Careri F, Monforti F, Huld T, Badger J. EMHIRES dataset. Part I: Wind power generation European Meteorological derived High resolution RES generation time series for present and future scenarios. 2016. doi:10.2790/831549.
- [22] Staffell I, Pfenninger S. Using bias-corrected reanalysis to simulate current and future wind power output. *Energy* 2016;114:1224–39. doi:10.1016/j.energy.2016.08.068.
- [23] Olauson J, Bergström H, Bergkvist M. Scenarios and time series of future wind power production in Sweden. Uppsala: 2015.
- [24] Olauson J, Bergkvist M. Modelling the Swedish wind power production using MERRA reanalysis data. *Renew Energy* 2015;76:717–25. doi:10.1016/j.renene.2014.11.085.
- [25] Global Modeling and Assimilation Office (GMAO). MERRA-2 const\_2d\_asm\_Nx: 2d, constants V5.12.4. Greenbelt, MD, USA: 2015. doi:10.5067/ME5QX6Q5IGGU.
- [26] Center for International Earth Science Information Network - CIESIN - Columbia University. Gridded Population of the World, Version 4 (GPWv4): Population Count Adjusted to Match 2015 Revision of UN WPP Country Totals. Palisades, NY: 2016. doi:10.7927/H4SF2T42.
- [27] Damm A, Köberl J, Prettenhaler F, Rogler N, Töglhofer C. Impacts of +2 °C global warming on electricity demand in Europe. *Clim Serv* 2017;7:12–30. doi:10.1016/j.cliser.2016.07.001.
- [28] Auffhammer M, Baylis P, Hausman CH. Climate change is projected to have severe impacts on the frequency and intensity of peak electricity demand across the United States. *Proc Natl Acad Sci* 2017;114:1886–91. doi:10.1073/pnas.1613193114.
- [29] Hyndman RJ, Fan S. Density Forecasting for Long-Term Peak Electricity Demand. *IEEE Trans Power Syst* 2010;25:1142–53. doi:10.1109/TPWRS.2009.2036017.
- [30] MIRASGEDIS S, SARAFIDIS Y, GEORGOPOULOU E, LALAS D, MOSCHOVITS M, KARAGIANNIS F, et al. Models for mid-term electricity demand forecasting incorporating weather influences. *Energy* 2006;31:208–27. doi:10.1016/j.energy.2005.02.016.
- [31] MAGNANO L, BOLAND J. Generation of synthetic sequences of electricity demand: Application in South Australia. *Energy* 2007;32:2230–43. doi:10.1016/j.energy.2007.04.001.
- [32] Svenska Kraftnät. Swedish Energy Market Data 2016. <https://www.svk.se/en/stakeholder-portal/Electricity-market/data-hub/> (accessed June 7, 2017).
- [33] Energiföretagen (Swedish Energy Companies). Power situation in Sweden - The Energy Year 2017. 2017.
- [34] Dujardin J, Kahl A, Krüyt B, Bartlett S, Lehning M. Interplay between photovoltaic, wind energy and storage hydropower in a fully renewable Switzerland. *Energy* 2017;135:513–25. doi:10.1016/j.energy.2017.06.092.
- [35] Holttinen H, Rissanen S, Larsen X, Løvholm AL. Wind and load variability in the Nordic countries.
- [36] Thornton HE, Scaife AA, Hoskins BJ, Brayshaw DJ. The relationship between wind power, electricity demand and winter weather patterns in Great Britain. *Environ Res Lett* 2017;12:064017. doi:10.1088/1748-9326/aa69c6.
- [37] Sinden G. Characteristics of the UK wind resource: Long-term patterns and relationship to electricity demand. *Energy Policy* 2007;35:112–27. doi:10.1016/j.enpol.2005.10.003.

- [38] Staffell I, Pfenninger S. The increasing impact of weather on electricity supply and demand. *Energy* 2018;145:65–78. doi:10.1016/j.energy.2017.12.051.
- [39] Liljeblad A. Future electricity use. Stockholm: The Royal Swedish Academy of Engineering Sciences (IVA); 2016.
- [40] Pfenninger S. Dealing with multiple decades of hourly wind and PV time series in energy models: A comparison of methods to reduce time resolution and the planning implications of inter-annual variability. *Appl Energy* 2017;197:1–13. doi:10.1016/j.apenergy.2017.03.051.
- [41] Collins S, Deane P, Ó Gallachóir B, Pfenninger S, Staffell I. Impacts of Inter-annual Wind and Solar Variations on the European Power System. *Joule* 2018;2:2076–90. doi:10.1016/j.joule.2018.06.020.
- [42] Vattenkraft.info. Swedish hydro power plant inventory 2016. <http://vattenkraft.info> (accessed June 7, 2017).

## 7 Appendix

### A1 Validation of simulated wind power time series with a focus on extreme events

In this section we assess the ability of the simulated wind power time series taken from Olauson et.al. [23] to reproduce historically observed extreme generation events. For the validation of hourly wind power generation we compare the simulated time series with historic generation for the years 2008, 2010 and 2012 in Sweden [32]. As the simulated time series provide capacity factors, while the observed generation is given in kWh, a time series of capacity factors is derived from the historic data, based on installed capacities. For the validation we assess capacity factor time series by means of basic model quality criteria, an evaluation of seasonal and hourly differences between model and observation values, and an assessment of events of extreme high and low generation events as well as ramps in generation.

Table A1: Table basic model quality criteria

	Hourly	Daily	Monthly
<b>Correlation</b>	0.974	0.988	0.995
<b>NRMSE</b>	0.160	0.102	0.033
<b>NMAE</b>	0.121	0.076	0.024
<b>n</b>	26328	1097	36

The model validation based on basic model quality criteria shows a good overall model fit, slight underestimation of frequencies of high generation events and an overestimation of low generation events. Table A1 summarizes basic model quality criteria, namely correlation, normalised root mean square error (NRMSE), and normalised mean absolute error (NMAE) and the number of events (n) within various time frames for the whole generation time series. Daily and monthly data are aggregates of hourly values.

The comparison of frequencies of different capacity factor bins of the simulated time series with historic values shows a slight overestimation of low capacity factors up to 0.1, a good fit of frequencies between 0.2 and 0.8 and underestimations of high modelled values above 0.8 (see figure A1).

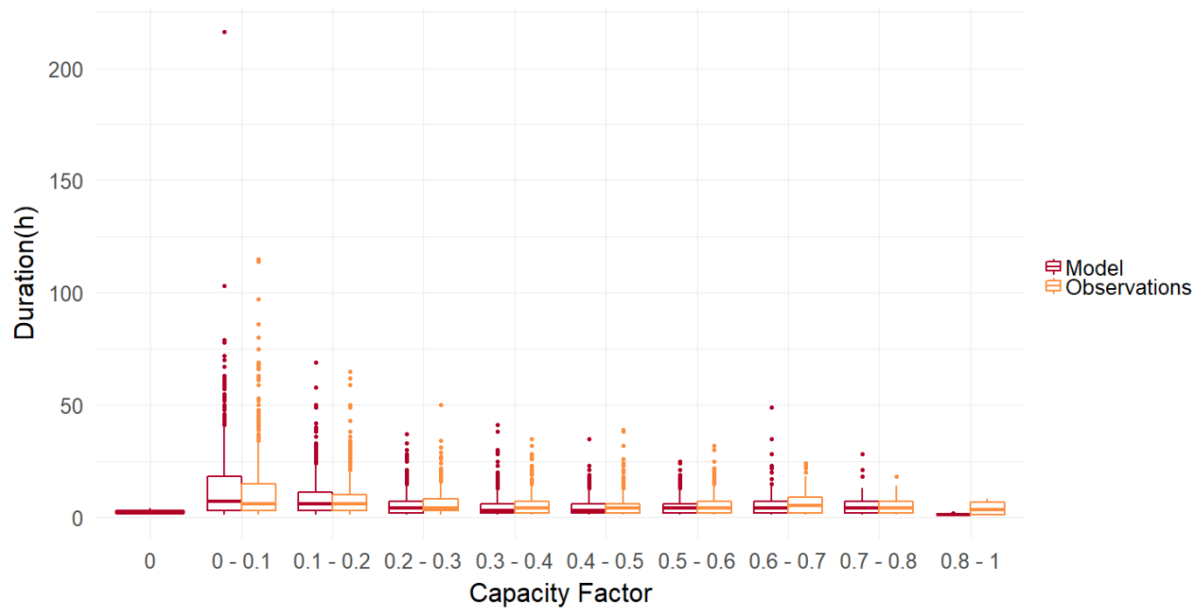


Figure A1: Frequency (hours per year) of simulated and observed historic values for different capacity factor classes

Table A2 and Table A3 show mean durations and frequencies of extreme generation events. The frequency of modelled low generation values (below 0.05 and below 0.025) and higher capacity factor values (above 0.6 and above 0.7) differs significantly between the modelled and observed values. The model overestimates the frequency of low production events, while it underestimates both average duration and the frequency of high production events with capacity factors of above 0.8. Additionally, it slightly overestimates the frequency and duration of persistent extreme events (longer than 24h) compared to the observations.

Table A2: Comparison of extreme generation events

		< 0.025	< 0.05	< 0.1	> 0.6	> 0.7	> 0.8
Model	Frequency	634	2130	6017	1321	309	5
	Mean duration	4.59	7.98	14.89	11.1	5.94	1.25
	Max. duration	28	73	216	60	28	2
Observations	Frequency	468	1826	5716	1125	248	16
	Mean duration	4.59	8.08	12.37	11.48	5.9	4
	Max duration	24	39	115	58	18	8

Table A3: Comparison of extreme generation events with a duration of more than 24 hours

		< 0.025	< 0.05	< 0.1	> 0.6	> 0.7
Model*	Frequency	1	18	74	13	1
	Mean duration	28	35.89	49.24	36.08	28
Observations*	Frequency	1	14	68	9	-
	Mean duration	24	31.57	45.88	31.78	-

\*no observation values for threshold above 0.7 and above 0.8; no model values above 0.8

Figure A2 compares frequencies and durations of low and high generation events for different capacity factor thresholds between modelled and observed values. The significance of some capacity factor thresholds may be questionable due to the low number of observations (i.e. for capacity factors above 0.8). In general, the duration of extreme events is overestimated with some minor exceptions (e.g. capacity factors above 0.8). Therefore, the simulated wind power time series provide a conservative estimate as the actual number of observed low wind generation events is likely to be lower, which would result in fewer extreme residual load events.

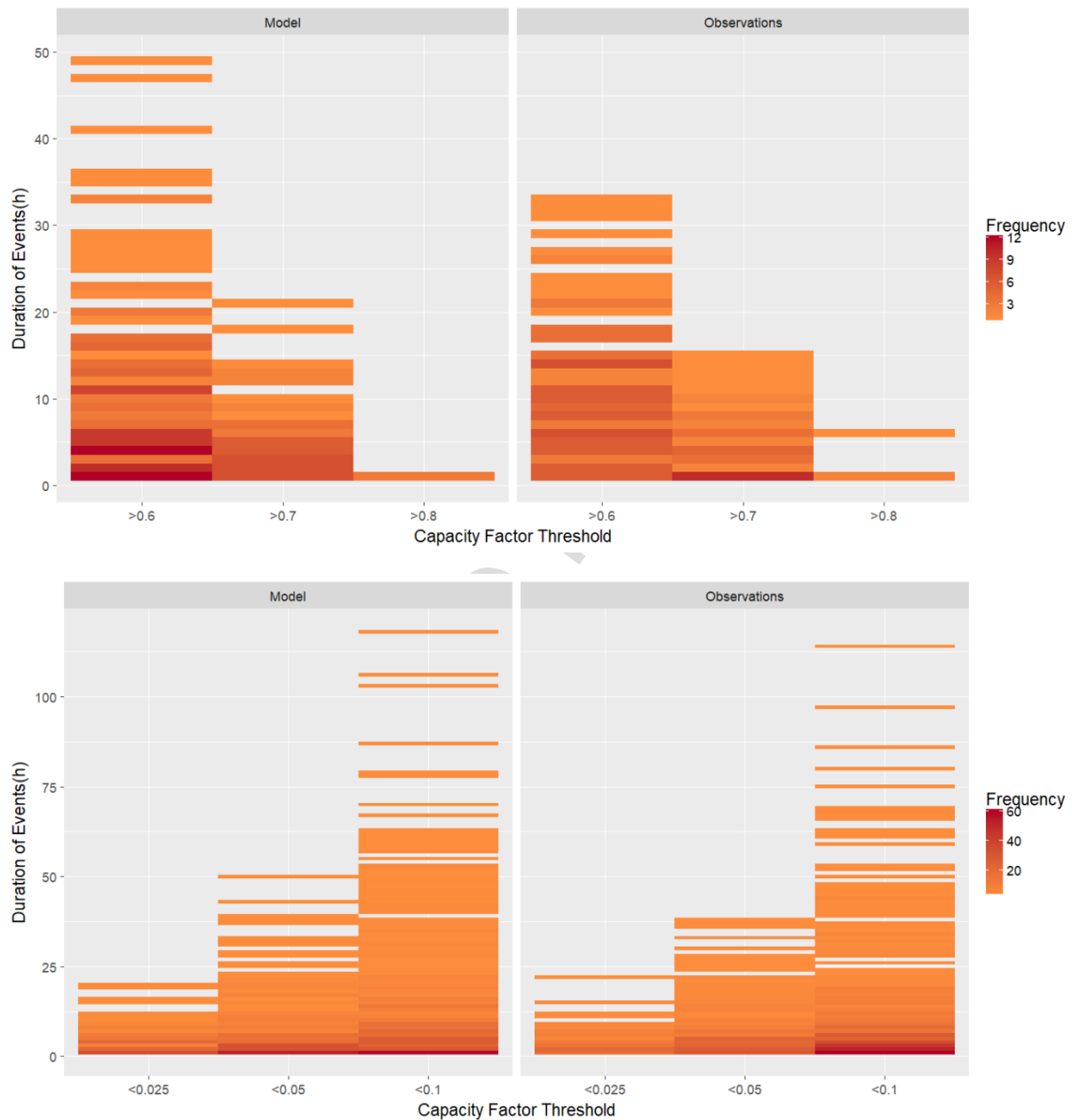


Figure A2: Comparison of durations and frequencies of high (above) and low (below) generation events in the simulated and the historically observed time series

## A2 The four bidding areas of the Swedish power market

The Swedish power market (Figure A3) is divided into four bidding areas: Luleå (SE1), Sundsvall (SE2), Stockholm (SE3) and Malmö (SE4). Figure A1 shows that the majority of electricity is consumed in the population rich Stockholm bidding area SE3, while demand in the northern regions SE1 and SE2 is relatively low. The borders between bidding areas have been drawn according to transmission limitations of the national grid [42]. Transmission bottlenecks result in different electricity prices between the bidding areas.

Currently, a large amount of electricity is transported from north to south, as the northern bidding areas generate a large electricity surplus due to their large hydro power resources (see Table A4). All of the existing nuclear power plants are located in SE3. They provide about 72 % of the electricity demand in the Stockholm area. Replacing nuclear power capacities by spatially more equally distributed wind and PV generation capacities would result in a larger power deficit in SE3. Contrarily, in the Malmö area (SE4), which now had the greatest deficit, new wind and PV capacities would allow production of more electricity than needed in the region. Overall, the proposed fully renewable power scenarios would intensify the current pattern with power surplus in the north and power deficit in the south (i.e. in SE3). This would further increase the pressure on the transmission power grid and investments into new transmission capacities are likely to be needed to avoid future bottlenecks.

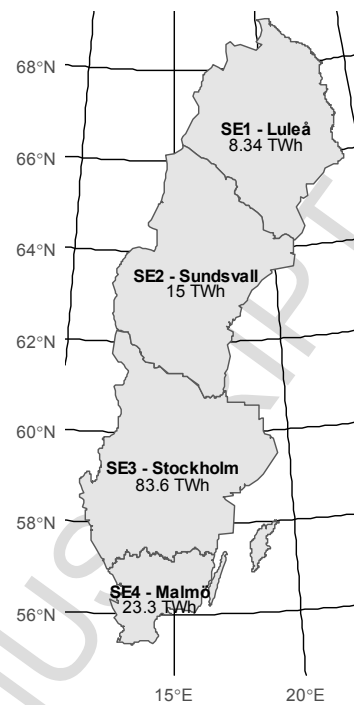


Figure A3: Mean annual electricity demand in the for Swedish bidding areas from 2010 to 2014



Table A4: Annual power generation and electricity demand in the four Swedish bidding areas for the three assessed scenarios (Reference, Wind, Wind+PV). Mean values for the period from 2010 to 2014 in TWh.

Scenario	Area	Generation					Demand	Difference
		hydro	nuclear	solar	thermal	wind	total	
Reference	SE1	18.78	0.00	0.00	0.26	0.64	19.68	11.33
Reference	SE2	36.31	0.00	0.00	0.84	1.56	38.71	23.67
Reference	SE3	11.42	60.33	0.00	5.65	3.18	80.58	-2.98
Reference	SE4	1.65	0.00	0.00	2.42	2.34	6.41	-16.93
Reference	sum	68.17	60.33	0.00	9.17	7.71	145.39	15.10
Wind	SE1	17.14	0.00	0.00	0.26	5.05	22.46	13.83
Wind	SE2	35.55	0.00	0.00	0.84	15.77	52.16	37.22
Wind	SE3	11.15	0.00	0.00	5.65	19.34	36.14	-47.35
Wind	SE4	0.67	0.00	0.00	2.42	29.31	32.40	9.12
Wind	sum	64.51	0.00	0.00	9.17	69.47	143.15	12.82
Wind+PV	SE1	17.14	0.00	0.00	0.26	4.85	22.25	13.62
Wind+PV	SE2	35.55	0.00	1.85	0.84	12.52	50.76	35.83
Wind+PV	SE3	11.15	0.00	10.36	5.65	15.88	43.04	-40.46
Wind+PV	SE4	0.67	0.00	2.87	2.42	21.23	27.19	3.92
Wind+PV	sum	64.51	0.00	15.09	9.17	54.48	143.25	12.92

### A3 Validation of simulated load with historic load data

For the long term evaluation of extreme residual load events we had to rely on simulated load time series as historic hourly load data is available only from 2007. Therefore, we applied a statistical model that uses population weighted mean temperature to simulate hourly load. In this section we demonstrate the ability of the model to reproduce historic load and its impact on assessing climatic extreme events. Figure A4 compares the monthly historic and simulated load. For the period from 2008 to 2014 the correlation of monthly loads is 0.991. The correlation of hourly loads for the same period is 0.963.

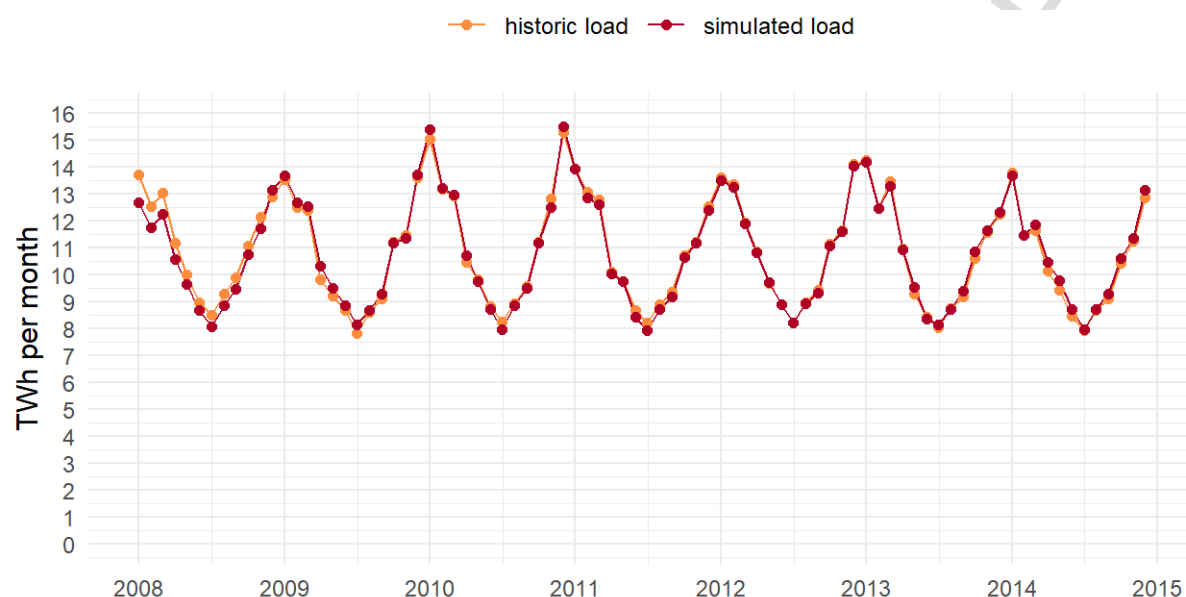


Figure A4: Monthly historic and simulated load from 2008 to 2014

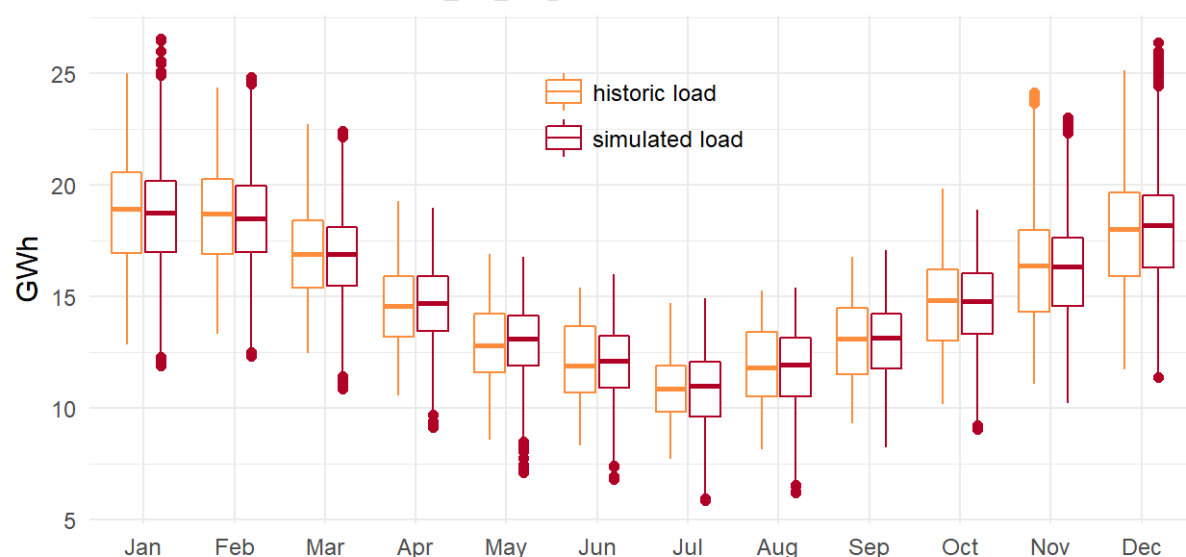


Figure A5: Distribution of historic and simulated hourly loads for all month from 2008 to 2014.

For our assessment of extreme residual load events it is crucial that extreme loads are captured sufficiently well. Figure A5 compares the distributions of hourly loads for all months. It shows that the simulated monthly mean values are on average about one percent lower than the historic values. With the exception of July, the standard deviation is also from one up to eight percent lower in the simulated time series. Contrarily, we observe more extremely low and high loads especially during winter, which affects our analysis of extreme residual loads the most. Figure A6 highlights that during residual load events the mean simulated load overestimates the actually observed historic load by 0.39 to 0.69 GW. Therefore, using simulated load time series may slightly overestimate the occurrence of extreme residual load events and the reported lack of capacity may be slightly lower due to the same effect.

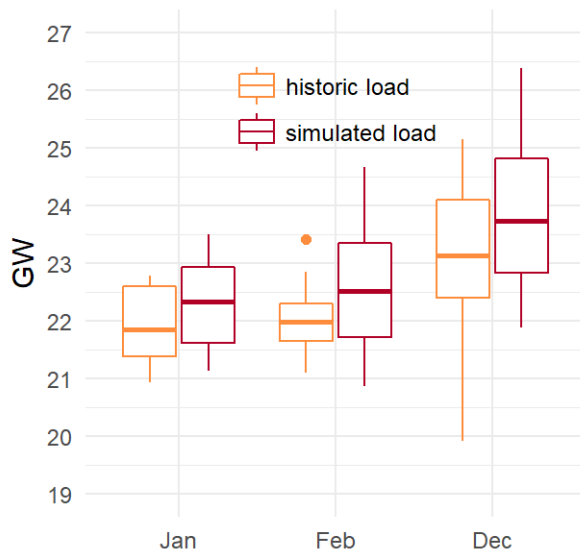


Figure A6: Distribution of historic and simulated hourly loads during extreme residual load events between 2008 and 2014

#### A4 Simulation and validation of hydro power generation time series

The Swedish version of the hydrological catchment model S-HYPE provides river discharge for 36,692 subbasins. The model simulates water flow from precipitation through soil, river and lakes to the river outlet [19,20] and provides daily time series of natural and corrected river runoff. The natural runoff simulates river runoff without human interference such as hydropower, while the corrected runoff incorporates historic hydropower generation and irrigation patterns.

To translate the time series on river discharge into time series of hydropower generation we used a spatially explicit data set of Swedish hydro power plants [42]. It contains information on the installed capacity and head height for about 1450 Swedish hydro power plants that allowed us to simulate hourly generation time series at plant level. For our analysis, we selected only plants with an installed capacity of more than 10 MW. This resulted in a data set of the 200 plants that together account for 95 % of the Swedish hydro power generation (see figure A7).

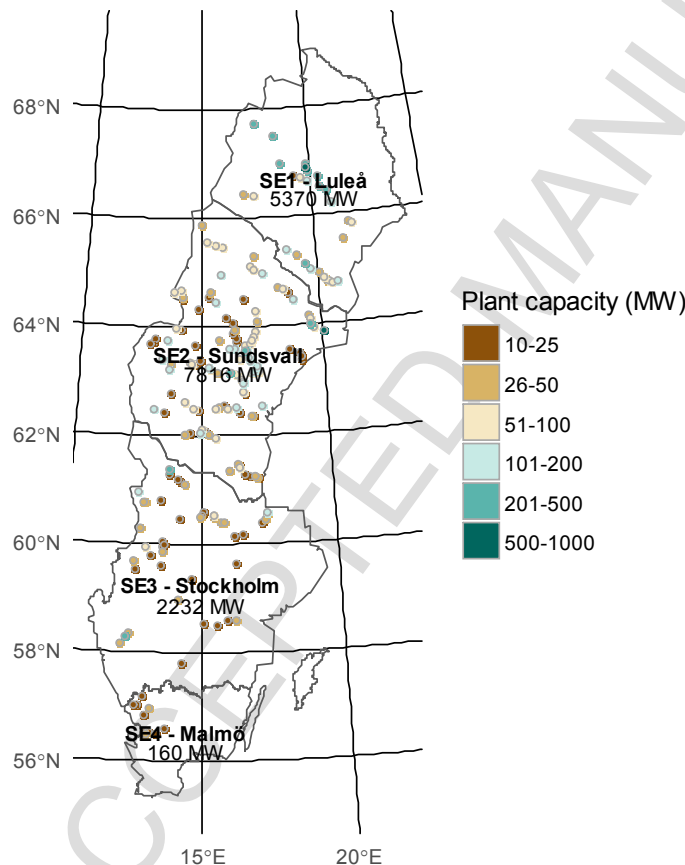


Figure A7: Cumulated hydro power capacity per bidding area and location and capacity of the 200 largest hydro power plants in Sweden that amount to 95 % of the total installed capacity and have been included in our analysis

The validation of our simulated hydro power generation time series against historic data demonstrates that the corrected S-HYPE time series cover seasonal and annual variations quite well. Simulated and historic monthly hydro power show a correlation of 0.94 in the period from 2008 to 2014 (see figure A8). After accounting for the fact that we included only 95 % of the generation capacities and adjusting the generation to 100 %, the average annual

power production is slightly overestimated by about 0.60 %. Overall, with the corrected S-HYPE time series and the spatially explicit hydro power data set it is possible to reproduce historic hydro power generation very well. However, due to the large storage capacities of Swedish hydro power plants, they can be operated very flexibly to respond to demand fluctuations or outages of other power plants. Therefore, the corrected S-HYPE time series, which already incorporates past hydro power generation and thus implicitly also the past power generation portfolios, are not applicable for assessing fundamentally different power mixes, as we do in our fully renewable power scenarios.

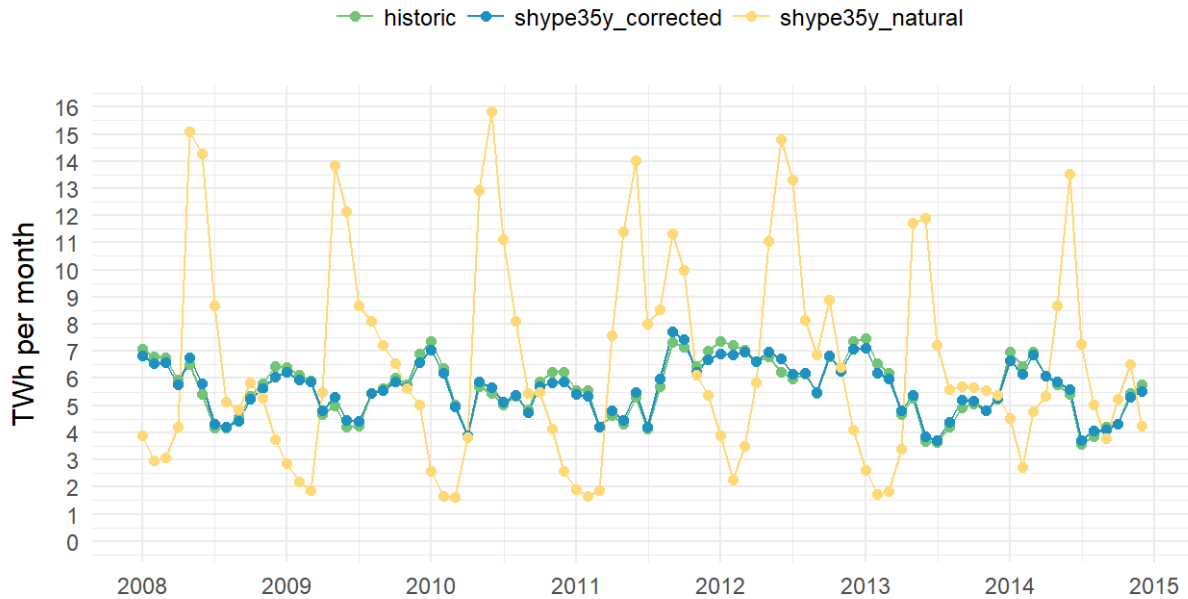


Figure A8: Monthly historic and simulated hydro power generation in TWh. The shype35y\_corrected time series accounts for the effect of historic hydro power generation on river runoff, while shype35y\_natural shows the theoretic hydro power generation without hydro reservoirs or any other human interference

For this task we use the S-HYPE natural runoff time series in an optimization model that adjusts hydro power generation so that the residual load balancing demand is minimized (see section 2.4). The aim of this approach is to allow hydro power generation to be adjusted flexibly to new residual load patterns that result from VRE fluctuations, while accounting for interannual and seasonal runoff variations and guaranteeing that operational restrictions are taken into account.

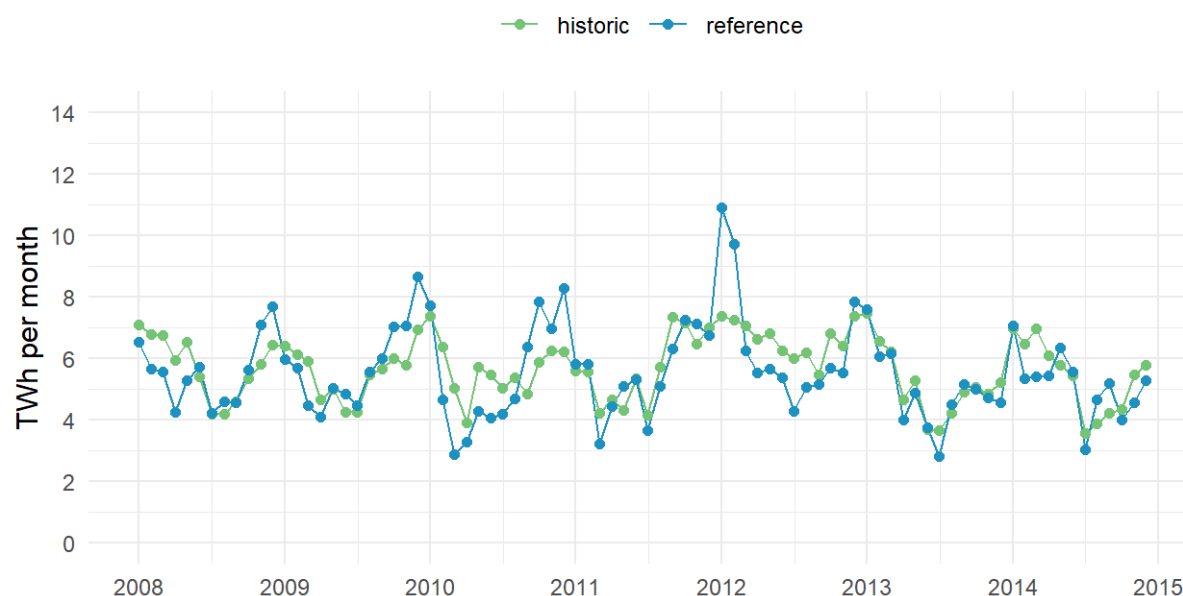


Figure A9: Monthly historic and optimized hydro power generation in the reference scenario. The historic hydro power generation [32] and the reference scenario time series is based on the optimization model for minimizing residual load demand.

The optimized hydro power generation in the reference scenario, which assumes historic generation capacities and load, should therefore look similar to the historically observed ones. The comparison of simulated and historic annual hydro power generation between 2008 and 2014 show a high correlation of 0.944 (Figure A9).

### A5 Sensitivity analyses of weight factors

We have assessed varying weight factors using the objective function. Figure A10 shows that the absolute levels of the weights do not matter, but the relative ranking does. E.g. when hydro weights grow higher than thermal weights (red-line at hydro weights of 2), thermal generation is increased. As long as hydro weights are equal to or lower than thermal weights, dispatch does not change. Even changing the weight for loss-of-load by an order of magnitude (from 10 to 100) does not change dispatch.

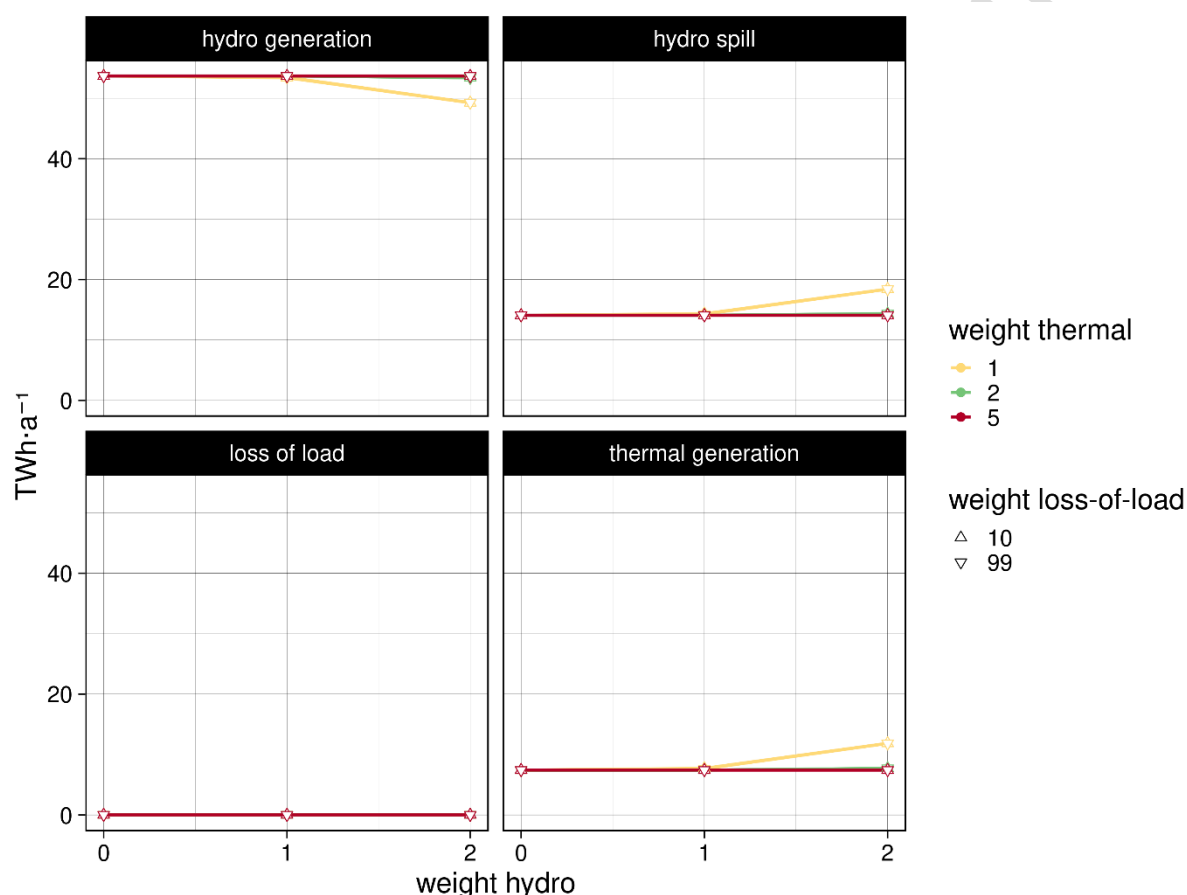


Figure A10: Sensitivity analysis of weight factors of the objective function